OPARC: Optimal and Precise Array Response Control Algorithm—Part I: Fundamentals

Xuejing Zhang, *Student Member, IEEE*, Zishu He, *Member, IEEE*, Xiang-Gen Xia, *Fellow, IEEE*, Bin Liao, *Senior Member, IEEE*, Xuepan Zhang, and Yue Yang, *Student Member, IEEE*

***Abstract*—In this paper, the problem of how to optimally and precisely control array response levels is addressed. By using the concept of the optimal weight vector from the adaptive array theory and adding virtual interferences one by one, the change rule of the optimal weight vector is found and a new formulation of the weight vector update is thus devised. Then, the issue of how to precisely control the response level of one single direction is investigated. More specifically, we assign a virtual interference to a direction such that the response level can be precisely controlled. Moreover, the parameters, such as the interference-to-noise ratio, can be figured out according to the desired level. Additionally, the parameter optimization is carried out to obtain the maximal array gain. The resulting scheme is called optimal and precise array response control (OPARC) in this paper. To understand it better, its properties are given, and its comparison with the existing accurate array response control algorithm is provided. Finally, simulation results are presented to verify the effectiveness and superiority of the proposed OPARC.**

***Index Terms*—Array response control, adaptive array theory, array pattern synthesis, array signal processing.**

I. Introduction

ARRAY antenna has been extensively applied in many fields, such as, radar, navigation and wireless communications [1]. It is known that the array pattern design is of significant importance to enhance system performance. For instance, in radar systems, it is desirable to mitigate returns from interfering signals, by designing a scheme which results in nulls at directions of interferences. In some communication systems, it is critical to shape multiple-beam patterns for multi-user reception. Additionally, synthesizing a pattern with broad mainlobe is beneficial to extend monitoring areas in satellite remote sensing. Generally speaking, array pattern can be designed either adaptively or non-adaptively. Determining the complex weights for array elements so as to achieve a desired beampattern is known as array pattern synthesis. With regard to this problem, it is expected to find weights that satisfy a set of specifications on a given beampattern, in a data-independent or nonadaptive manner.

Over the past several decades, a great number of pattern synthesis approaches have been proposed, see, e.g., [2]–[14]. Particularly, in [12], an iterative sampling method is utilized to make the sidelobe peaks conform to a specified shape within a given tolerance. For sidelobe control in cylindrical arrays, an artificially created noise source environment can be utilized [13]. For a circular ring array, a symmetrical pattern with low sidelobes is achieved in [14] by adopting a field-synthesis technique. Note that although the solutions in [12]–[14] are able to control sidelobes for arrays with some particular configurations, they cannot be straightforwardly extended to general geometries. On the contrary, the accurate array response control (A^2RC) approach [15] provides a simple and effective manner to accurately control array response level of arbitrary arrays. The A^2RC algorithm stems from the adaptive array theory. Unfortunately, the weight update of A^2RC is theoretically imperfect and the ultimate result may suffer from a performance loss, see [16]. Based on A^2RC, a multi-point accurate array response control (MA^2RC) method has been developed in [17] to flexibly adjust array responses of multiple points. However, a satisfactory performance cannot be always guaranteed due to its empirical solution.

These shortcomings of the existing approaches motivate us to have an innovative method to precisely, flexibly and optimally control the response level. To do so, we first investigate how the optimal weight vector in the adaptive array theory changes along with the increase of the number of interferences. Then, a new scheme for weight vector update is developed and further exploited to realize the precise array response control. Furthermore, a parameter optimization mechanism is proposed by maximizing the array gain [18]. It is shown that, the proposed optimal and precise array response control (OPARC) algorithm is capable of precisely and flexibly controlling the response level of an arbitrary array. Furthermore, its optimality (in the sense of array gain) can be well guaranteed. Although it is also

Manuscript received December 26, 2017; revised May 20, 2018 and September 17, 2018; accepted November 25, 2018. Date of publication December 7, 2018; date of current version December 18, 2018. The associate editor coordinating the review of this manuscript and approving it for publication was Dr. Pengfei Xia. This work was supported in part by the National Nature Science Foundation of China under Grants 61671139, 61671137, 61771316, and 61701499; in part by the Foundation of Shenzhen under Grant JCYJ20170302150044331; and in part by the China Scholarship Council. *(Corresponding author: Xuejing Zhang.)*

Xuejing Zhang is with the University of Electronic Science and Technology of China, Chengdu 611731, China, and also with the Department of Electrical and Computer Engineering, University of Delaware, Newark, DE 19716 USA (e-mail: xjzhang7@163.com).

Z. He and Y. Yang are with the University of Electronic Science and Technology of China, Chengdu 611731, China (e-mail: zshe@uestc.edu.cn; yueyang@std.uestc.edu.cn).

X.-G. Xia is with the Department of Electrical and Computer Engineering, University of Delaware, Newark, DE 19716 USA (e-mail: xxia@ee.udel.edu).

B. Liao is with the College of Information Engineering, Shenzhen University, Shenzhen 518060, China (e-mail: binliao@szu.edu.cn).

Xuepan Zhang is with the Qian Xuesen Laboratory of Space Technology, Beijing 100094, China (e-mail: zhangxuepan@qxslab.cn).

Digital Object Identifier 10.1109/TSP.2018.2885454

developed from the foundation of the adaptive array theory, the resulting weight vector of the proposed OPARC algorithm is an optimal beamformer, which may not be true in the existing A^{2}RC method. More specific differences between OPARC and A^{2}RC will be presented later.

It should be mentioned that this paper focuses on the main concepts and fundamentals of the OPARC scheme, while the extensions and applications (such as pattern synthesis and quiescent pattern control [19]) will be carried out in the companion paper [20]. The rest of the paper is organized as follows. Our proposed OPARC algorithm is presented in Section II. Further insights into OPARC are presented in Section III to provide more useful and interesting properties. In Section IV, comparisons between OPARC and the existing A^{2}RC are presented. Representative simulations are conducted in Section V and conclusions are drawn in Section VI.

Notations: We use bold upper-case and lower-case letters to represent matrices and vectors, respectively. In particular, we use $\mathbf{I}$, $\mathbf{1}$ and $\mathbf{0}$ to denote the identity matrix, the all-one vector and the all-zero vector, respectively. $j \triangleq \sqrt{-1}$. $(\cdot)^{\mathrm{T}}$, $(\cdot)^*$ and $(\cdot)^{\mathrm{H}}$ stand for the transpose, complex conjugate and Hermitian transpose, respectively. $|\cdot|$ denotes the absolute value and $\|\cdot\|_2$ denotes the l_2 norm. We use $\mathbf{H}(i,l)$ to stand for the element at the ith row and lth column of matrix $\mathbf{H}$. $\Re(\cdot)$ and $\Im(\cdot)$ denote the real and imaginary parts, respectively. $E\{\cdot\}$ represents expectation. $\det(\cdot)$ is the determinant of a matrix. The sign function is denoted by $\mathrm{sign}(\cdot)$. $\oslash$ represents the element-wise division operator. We use $\mathrm{diag}(\cdot)$ to return a column vector composed of the diagonal elements of a matrix, and use $\mathrm{Diag}(\cdot)$ to stand for the diagonal matrix with the components of the input vector as the diagonal elements. Finally, $\mathbb{R}$ and $\mathbb{C}$ denote the sets of all real and all complex numbers, respectively, and $\mathbb{S}_{++}^N$ denotes the set of $N \times N$ positive definite matrices.

II. OPARC Algorithm

In order to present our proposed OPARC algorithm, we first briefly recall the adaptive array theory.

A. Adaptive Array Theory

Consider an array of N elements. The array observation vector $\mathbf{x}(t)$, which is composed of the components of signal, interference and noise, can be expressed as

$$\mathbf{x}(t) = \mathbf{a}(\theta_0)s_0(t) + \sum_{\ell=1}^{k} \mathbf{a}(\theta_\ell)s_\ell(t) + \mathbf{n}(t) \tag{1}$$

where $\mathbf{n}(t)$ stands for the noise component, k is the number of interferences, θ_0 is the angle of the desired signal, $s_0(t)$ is the signal waveform, θ_ℓ and $s_\ell(t)$ denote the angle and waveform of the ℓth interference, respectively, $\ell = 1, \ldots, k$. In addition, $\mathbf{a}(\theta)$ represents the steering vector.[1] More exactly, for a given θ, we have

$$\mathbf{a}(\theta) = [g_1(\theta)e^{-j\omega\tau_1(\theta)}, \ldots, g_N(\theta)e^{-j\omega\tau_N(\theta)}]^{\mathrm{T}} \tag{2}$$

where $g_n(\theta)$ denotes the pattern of the nth element, $\tau_n(\theta)$ is the time-delay between the nth element and the reference point, $n = 1, \ldots, N$, ω denotes the operating frequency. Assuming that the noise is white and the interferences are independent with each other, we can express the $N \times N$ noise-plus-interference covariance matrix as

$$\begin{aligned}\mathbf{R}_{n+i} &= E\left\{\left(\sum_{\ell=1}^{k}\mathbf{a}(\theta_\ell)s_\ell(t)+\mathbf{n}(t)\right)\left(\sum_{\ell=1}^{k}\mathbf{a}(\theta_\ell)s_\ell(t)+\mathbf{n}(t)\right)^{\mathrm{H}}\right\} \\ &= \sigma_n^2\mathbf{I} + \sum_{\ell=1}^{k}\sigma_\ell^2\mathbf{a}(\theta_\ell)\mathbf{a}^{\mathrm{H}}(\theta_\ell)\end{aligned} \tag{3}$$

where σ_n^2 and σ_ℓ^2 stand for the noise and interference powers, respectively.

The output of a narrow band beamformer is given by

$$y(t) = \mathbf{w}^{\mathrm{H}}\mathbf{x}(t) \tag{4}$$

where t is the time index, $\mathbf{w}$ is the $N \times 1$ complex vector of beamformer weights. To suppress the unwanted interferences and noise, the optimal adaptive beamformer weight vector $\mathbf{w}$ steering to the direction θ_0 can be obtained by maximizing the output signal-to-interference-plus-noise ratio (SINR) defined as

$$\mathrm{SINR} = \frac{\sigma_s^2|\mathbf{w}^{\mathrm{H}}\mathbf{a}(\theta_0)|^2}{\mathbf{w}^{\mathrm{H}}\mathbf{R}_{n+i}\mathbf{w}} \tag{5}$$

where $\sigma_s^2 = E\{|s_0(t)|^2\}$ stands for the signal power. It is known that the optimal weight vector $\mathbf{w}_{\mathrm{opt}}$, which maximizes the SINR, is given by [18]

$$\mathbf{w}_{\mathrm{opt}} = \alpha\mathbf{R}_{n+i}^{-1}\mathbf{a}(\theta_0) \tag{6}$$

where α is a normalization factor and does not affect the output SINR, and hence, will be omitted in the sequel.

Note that the above SINR can be expressed as $G \cdot \sigma_s^2/\sigma_n^2$, where G is defined as

$$G = \frac{|\mathbf{w}^{\mathrm{H}}\mathbf{a}(\theta_0)|^2}{\mathbf{w}^{\mathrm{H}}\mathbf{T}_{n+i}\mathbf{w}} \tag{7}$$

with $\mathbf{T}_{n+i} \triangleq \mathbf{R}_{n+i}/\sigma_n^2$ standing for the normalized noise-plus-interference covariance matrix, i.e.,

$$\mathbf{T}_{n+i} = \frac{\mathbf{R}_{n+i}}{\sigma_n^2} = \mathbf{I} + \sum_{\ell=1}^{k}\beta_\ell\mathbf{a}(\theta_\ell)\mathbf{a}^{\mathrm{H}}(\theta_\ell) \tag{8}$$

where $\beta_\ell \triangleq \sigma_\ell^2/\sigma_n^2$ denotes the interference-to-noise ratio (INR). Note that G represents the amplification factor of the input signal-to-noise ratio (SNR) σ_s^2/σ_n^2, and therefore, is termed as the array gain [18]. As a result, the criterion of array gain G maximization is adopted to achieve the optimal weight vector.

B. Update of the Optimal Weight Vector

It can be seen from (6)–(8) that the optimal weight vector $\mathbf{w}_{\mathrm{opt}}$ depends on $\mathbf{R}_{n+i}$ or $\mathbf{T}_{n+i}$, which is not available for the following data-independent array response control: for

[1]Note that in this work, we reasonably assume that the steering vector $\mathbf{a}(\theta)$ is known exactly, also see in [10]–[12]. Otherwise, we should first estimate the steering vector and then apply our algorithm. The discussion of steering vector estimation is beyond the scope of this paper and the related study is not presented here.

a given steering vector $\mathbf{a}(\theta)$ in (2) and a beam axis θ_0, design a weight vector $\mathbf{w}$ such that the normalized array response $L(\theta,\theta_0) \triangleq |\mathbf{w}^{\mathrm{H}}\mathbf{a}(\theta)|^2/|\mathbf{w}^{\mathrm{H}}\mathbf{a}(\theta_0)|^2$ meets some specific requirements. In this paper, we are interested in the requirements of array response levels, i.e., finding weight vectors such that the array responses at a given set of angles are equal to a set of predescribed values. Our basic idea is to construct a virtual normalized noise-plus-interference covariance matrix (VCM), denoted as $\mathbf{T}_k$, to achieve the given response control task. Note that since the VCM $\mathbf{T}_k$ to be determined is not produced by real data, it may not have any physical meaning. Moreover, it can be neither positive definite nor Hermitian (its rationality will be discussed later). By making use of the VCM, the data-dependent adaptive array theory can be applied to the data-independent situation considered in this paper. This allows us to optimally update the weight vector $\mathbf{w}_{k-1,\mathrm{opt}} = \mathbf{T}_{k-1}^{-1}\mathbf{a}(\theta_0)$ to $\mathbf{w}_{k,\mathrm{opt}}$ such that a desired response level ρ_k at θ_k can be achieved by assigning an appropriate virtual interference. Thus, the problem we concern here is to figure out the characteristics, e.g., INR, of the virtual interference.

We use induction to describe the problem and the algorithm below. Suppose that the response levels of the $k-1$ directions have been successively controlled by adding $k-1$ virtual interferences. Meanwhile, the corresponding VCM is denoted as $\mathbf{T}_{k-1}$. For a given θ_k and its desired level ρ_k, we can assign the kth virtual interference coming from θ_k by designing its INR (i.e., β_k). To find out β_k, from (8) we notice that the VCM can be updated as

$$\mathbf{T}_k = \mathbf{T}_{k-1} + \beta_k \mathbf{a}(\theta_k)\mathbf{a}^{\mathrm{H}}(\theta_k). \tag{9}$$

Using the Woodbury Lemma [21], we have

$$\mathbf{T}_k^{-1} = \mathbf{T}_{k-1}^{-1} - \frac{\beta_k \mathbf{T}_{k-1}^{-1}\mathbf{a}(\theta_k)\mathbf{a}^{\mathrm{H}}(\theta_k)\mathbf{T}_{k-1}^{-1}}{1+\beta_k \mathbf{a}^{\mathrm{H}}(\theta_k)\mathbf{T}_{k-1}^{-1}\mathbf{a}(\theta_k)}. \tag{10}$$

Accordingly, the optimal weight vector is given by $\mathbf{w}_{k,\mathrm{opt}} = \mathbf{T}_k^{-1}\mathbf{a}(\theta_0)$. Recalling (6) and (10), we can express $\mathbf{w}_{k,\mathrm{opt}}$ as

$$\mathbf{w}_{k,\mathrm{opt}} = \mathbf{w}_{k-1,\mathrm{opt}} + \gamma_k \mathbf{T}_{k-1}^{-1}\mathbf{a}(\theta_k) \tag{11}$$

where $\mathbf{w}_{k-1,\mathrm{opt}} = \mathbf{T}_{k-1}^{-1}\mathbf{a}(\theta_0)$ denotes the previous optimal weight vector and γ_k is given by

$$\gamma_k = -\frac{\beta_k \mathbf{a}^{\mathrm{H}}(\theta_k)\mathbf{T}_{k-1}^{-1}\mathbf{a}(\theta_0)}{1+\beta_k \mathbf{a}^{\mathrm{H}}(\theta_k)\mathbf{T}_{k-1}^{-1}\mathbf{a}(\theta_k)} \triangleq \Psi_k(\beta_k) \tag{12}$$

with $\Psi_k(\cdot)$ denoting a mapping from β_k to γ_k.

Note that the solution in (11)–(12) gives the optimal solution for maximizing the SINR, which may not meet the response level ρ_k at θ_k. In order to meet this response level requirement, we next consider the following questions first. Given the previous weight vector $\mathbf{w}_{k-1,\mathrm{opt}} = \mathbf{T}_{k-1}^{-1}\mathbf{a}(\theta_0)$, does there exist γ_k (or equivalently β_k) such that the response level at θ_k is precisely ρ_k? and what value it should be if it exists? To do so, we reformulate the weight vector as

$$\mathbf{w}_k = \mathbf{w}_{k-1} + \gamma_k \mathbf{v}_k \tag{13}$$

where the subscript $(\cdot)_{\mathrm{opt}}$ is omitted for notational simplicity and $\mathbf{v}_k$ is defined as

$$\mathbf{v}_k \triangleq \mathbf{T}_{k-1}^{-1}\mathbf{a}(\theta_k). \tag{14}$$

Mathematically, the problem of finding γ_k such that the array response level at θ_k is ρ_k can be written as

$$L(\theta_k,\theta_0) = |\mathbf{w}_k^{\mathrm{H}}\mathbf{a}(\theta_k)|^2/|\mathbf{w}_k^{\mathrm{H}}\mathbf{a}(\theta_0)|^2 = \rho_k \tag{15}$$

where the desired array response level satisfies $\rho_k \le 1$. The combination of (13) and (15) yields

$$\mathbf{z}_k^{\mathrm{H}}\mathbf{H}_k\mathbf{z}_k = 0 \tag{16}$$

where $\mathbf{z}_k$ and $\mathbf{H}_k$ are, respectively, defined as

$$\begin{aligned}\mathbf{z}_k &\triangleq [1\ \gamma_k]^{\mathrm{T}}\\ \mathbf{H}_k &\triangleq [\mathbf{w}_{k-1}\ \mathbf{v}_k]^{\mathrm{H}}\left(\mathbf{a}(\theta_k)\mathbf{a}^{\mathrm{H}}(\theta_k) - \rho_k\mathbf{a}(\theta_0)\mathbf{a}^{\mathrm{H}}(\theta_0)\right)[\mathbf{w}_{k-1}\mathbf{v}_k].\end{aligned} \tag{17}$$

By expanding (16) and (17), we immediately have the following proposition.

Proposition 1: Suppose that γ_k (i.e., the second entry of $\mathbf{z}_k$) satisfies (16), if $\mathbf{H}_k(2,2) = 0$, it can be derived that the trajectory of $\left[\Re(\gamma_k)\ \Im(\gamma_k)\right]^{\mathrm{T}}$ is a line as

$$\Re[\mathbf{H}_k(1,2)]\Re(\gamma_k) - \Im[\mathbf{H}_k(1,2)]\Im(\gamma_k) = -\mathbf{H}_k(1,1)/2.$$

If $\mathbf{H}_k(2,2) \neq 0$, the trajectory of $[\Re(\gamma_k)\ \Im(\gamma_k)]^{\mathrm{T}}$ is a circle, denoted by $\mathbb{C}_\gamma$:

$$\mathbb{C}_\gamma = \left\{ [\Re(\gamma_k)\ \Im(\gamma_k)]^{\mathrm{T}} \,\middle|\, \left\| [\Re(\gamma_k)\ \Im(\gamma_k)]^{\mathrm{T}} - \mathbf{c}_\gamma \right\|_2 = R_\gamma \right\}$$

with the center

$$\mathbf{c}_\gamma = \frac{1}{\mathbf{H}_k(2,2)}\begin{bmatrix} -\Re\left[\mathbf{H}_k(1,2)\right] \\ \Im\left[\mathbf{H}_k(1,2)\right] \end{bmatrix} \tag{18}$$

and the radius

$$R_\gamma = \sqrt{-\det(\mathbf{H}_k)}/|\mathbf{H}_k(2,2)|. \tag{19}$$

Proof: See Appendix A. ■

From this proposition, it is known that, given the previous weight vector $\mathbf{w}_{k-1} = \mathbf{T}_{k-1}^{-1}\mathbf{a}(\theta_0)$, there exist infinitely many solutions of γ_k to achieve a response level of ρ_k at θ_k. This implies that the response level at a certain direction can be precisely adjusted by assigning a virtual interference with properly designed INR parameter γ_k.

It is clear that $\mathbf{H}_k(2,2) = 0$ is equivalent to

$$\rho_k = \frac{\left|(\mathbf{T}_{k-1}^{-1}\mathbf{a}(\theta_k))^{\mathrm{H}}\mathbf{a}(\theta_k)\right|^2}{\left|(\mathbf{T}_{k-1}^{-1}\mathbf{a}(\theta_k))^{\mathrm{H}}\mathbf{a}(\theta_0)\right|^2}. \tag{20}$$

In this case ρ_k is equal to the normalized power response at θ_k when the weight vector is $\mathbf{T}_{k-1}^{-1}\mathbf{a}(\theta_k)$, i.e., when the beampattern steers to the beam axis θ_k. Typically, a beampattern reaches its maximum at the beam axis, i.e., we have $\rho_k > 1$ if $\theta_k \neq \theta_0$. This would contradict with the fact that $\rho_k \le 1$. Hence, $\mathbf{H}_k(2,2) = 0$ usually will not occur and in the sequel we only focus on the case of $\mathbf{H}_k(2,2) \neq 0$, and from Proposition 1, the trajectory of $[\Re(\gamma_k)\,\Im(\gamma_k)]^{\mathrm{T}}$ is a circle, as illustrated in Fig. 1. Then, the remaining question is among all these valid solutions of γ_k (or β_k), to meet the response level requirement, which one is to

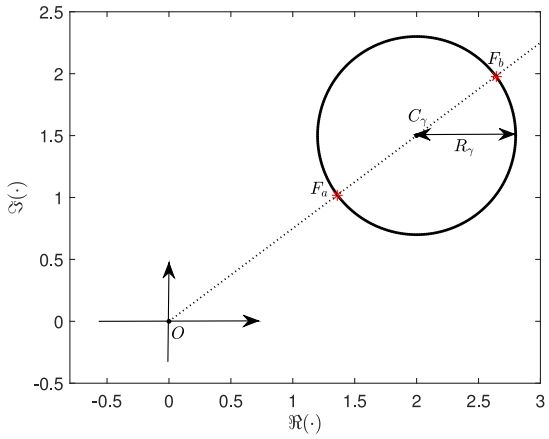

Fig. 1. Geometric distribution of γ_k (F_a and F_b represent the locations of $[\Re(\gamma_{k,a})\,\Im(\gamma_{k,a})]^{\mathrm{T}}$ and $[\Re(\gamma_{k,b})\,\Im(\gamma_{k,b})]^{\mathrm{T}}$, respectively).

maximize the SINR or beam gain? We will study this question below.

Remark 1: Note that in (13), a term has been added on the weight vector $\mathbf{w}_{k-1}$, and hence, the array power response at the beam axis θ_0 may change. This may degrade the performance on target detection. To this end, in the following, we maximize the array gain when controlling response level. Since the array gain is proportional to the output SINR, a good performance on target detection can thus be guaranteed.

C. Selection of γ_k and Update of the Weight Vector

The preceding problem can be formulated as the following constrained optimal and precise array response control (OPARC) problem:

$$\underset{\gamma_k}{\text{maximize}} \quad G_k \triangleq |\mathbf{w}_k^{\mathrm{H}}\mathbf{a}(\theta_0)|^2/|\mathbf{w}_k^{\mathrm{H}}\mathbf{T}_k\mathbf{w}_k| \tag{21a}$$

$$\text{subject to} \quad L(\theta_k,\theta_0)=\rho_k \tag{21b}$$

$$\mathbf{w}_k=\mathbf{w}_{k-1}+\gamma_k\mathbf{T}_{k-1}^{-1}\mathbf{a}(\theta_k). \tag{21c}$$

From (21a), one can see that the desired weight vector is expected to provide the maximum array gain with some additional constraints. Apart from the response level constraint (21b), we have also imposed constraint (21c) in the above OPARC scheme. This makes the resulting $\mathbf{w}_k$ be an optimal weight vector.

When γ_k satisfies (12), (21c) leads to $\mathbf{w}_k=\mathbf{T}_k^{-1}\mathbf{a}(\theta_0)$. In order to solve problem (21), we first substitute $\mathbf{w}_k=\mathbf{T}_k^{-1}\mathbf{a}(\theta_0)$ into the objective function and get

$$\begin{aligned} G_k &= \frac{\mathbf{a}^{\mathrm{H}}(\theta_0)\mathbf{T}_k^{-\mathrm{H}}\mathbf{a}(\theta_0)\mathbf{a}^{\mathrm{H}}(\theta_0)\mathbf{T}_k^{-1}\mathbf{a}(\theta_0)}{\left|\mathbf{a}^{\mathrm{H}}(\theta_0)\mathbf{T}_k^{-\mathrm{H}}\mathbf{T}_k\mathbf{T}_k^{-1}\mathbf{a}(\theta_0)\right|} \\ &= |\mathbf{a}^{\mathrm{H}}(\theta_0)\mathbf{T}_k^{-1}\mathbf{a}(\theta_0)| \end{aligned} \tag{22}$$

where we have utilized the identities $(\mathbf{a}^{\mathrm{H}}(\theta_0)\mathbf{T}_k^{-\mathrm{H}}\mathbf{a}(\theta_0))^{\mathrm{H}}=\mathbf{a}^{\mathrm{H}}(\theta_0)\mathbf{T}_k^{-1}\mathbf{a}(\theta_0)$ and $|\mathbf{a}^{\mathrm{H}}(\theta_0)\mathbf{T}_k^{-\mathrm{H}}\mathbf{a}(\theta_0)|=|\mathbf{a}^{\mathrm{H}}(\theta_0)\mathbf{T}_k^{-1}\mathbf{a}(\theta_0)|$. Note again that $\mathbf{T}_k$ is not assumed to be Hermitian symmetric in the derivation of (22). Then, recalling (10) and (12), we can rewrite G_k as

$$\begin{aligned} G_k &= \left|\mathbf{a}^{\mathrm{H}}(\theta_0)\mathbf{T}_{k-1}^{-1}\mathbf{a}(\theta_0)+\gamma_k\mathbf{a}^{\mathrm{H}}(\theta_0)\mathbf{T}_{k-1}^{-1}\mathbf{a}(\theta_k)\right| \\ &= |\widetilde{\xi}_c|\cdot|\xi_0/\widetilde{\xi}_c+\gamma_k| \end{aligned} \tag{23}$$

where ξ_0, ξ_k, ξ_c and $\widetilde{\xi}_c$ are defined as

$$\xi_0 \triangleq \mathbf{a}^{\mathrm{H}}(\theta_0)\mathbf{T}_{k-1}^{-1}\mathbf{a}(\theta_0) \tag{24a}$$

$$\xi_k \triangleq \mathbf{a}^{\mathrm{H}}(\theta_k)\mathbf{T}_{k-1}^{-1}\mathbf{a}(\theta_k) \tag{24b}$$

$$\xi_c \triangleq \mathbf{a}^{\mathrm{H}}(\theta_k)\mathbf{T}_{k-1}^{-1}\mathbf{a}(\theta_0) \tag{24c}$$

$$\widetilde{\xi}_c \triangleq \mathbf{a}^{\mathrm{H}}(\theta_0)\mathbf{T}_{k-1}^{-1}\mathbf{a}(\theta_k). \tag{24d}$$

Then, from Proposition 1, problem (21) can be expressed as

$$\underset{\gamma_k}{\text{maximize}} \quad |\xi_0/\widetilde{\xi}_c+\gamma_k| \tag{25a}$$

$$\text{subject to} \quad \left[\Re(\gamma_k)\;\Im(\gamma_k)\right]^{\mathrm{T}}\in\mathbb{C}_\gamma. \tag{25b}$$

Although the problem (25) is non-convex, it will be shown that it can be analytically solved as follows.

Proposition 2: Denote the intersections of the circle and the line connecting the origin $\mathbf{O}=[0,0]^{\mathrm{T}}$ and the center $\mathbf{c}_\gamma$ in (18) as $F_a \triangleq [\Re(\gamma_{k,a})\,\Im(\gamma_{k,a})]^{\mathrm{T}}$ and $F_b \triangleq [\Re(\gamma_{k,b})\,\Im(\gamma_{k,b})]^{\mathrm{T}}$, respectively, and assume that $|\gamma_{k,a}|<|\gamma_{k,b}|$. If $\mathbf{T}_{k-1}$ is Hermitian (note that the Hermitian property of $\mathbf{T}_{k-1}$ has not been guaranteed as we have mentioned earlier), then the optimal solution of (25) satisfies

$$\gamma_{k,\star}=\begin{cases}\gamma_{k,a}, & \text{if}\,\zeta>0\\ \gamma_{k,b}, & \text{otherwise}\end{cases} \tag{26}$$

where

$$\zeta \triangleq \mathrm{sign}[\mathbf{c}_\gamma(1)]\cdot\mathrm{sign}[\Re(d)-\mathbf{c}_\gamma(1)] \tag{27}$$

and

$$d \triangleq -\xi_0/\xi_c^*. \tag{28}$$

In addition, $\gamma_{k,a}$ and $\gamma_{k,b}$ in (26) are calculated as

$$\gamma_{k,a}=-\frac{(\|\mathbf{c}_\gamma\|_2-R_\gamma)\,\chi\xi_c}{\|\mathbf{c}_\gamma\|_2\mathbf{H}_k(2,2)},\ \gamma_{k,b}=-\frac{(\|\mathbf{c}_\gamma\|_2+R_\gamma)\,\chi\xi_c}{\|\mathbf{c}_\gamma\|_2\mathbf{H}_k(2,2)}$$

where $\chi=\xi_k-\rho_k\xi_0\in\mathbb{R}$, $\mathbf{c}_\gamma$ and R_γ are defined in Proposition 1.

Proof: See Appendix B. ■

To have a better understanding, the locations of $\gamma_{k,a}$ and $\gamma_{k,b}$ have been illustrated in Fig. 1. Obviously, once the optimal $\gamma_{k,\star}$ has been obtained, we can update the weight vector as

$$\mathbf{w}_k=\mathbf{w}_{k-1}+\gamma_{k,\star}\mathbf{v}_k. \tag{29}$$

This completes the update of weight vector of the kth step.

D. Update of the Inversion of VCM

Since the calculation of $\gamma_{k,\star}$ requires the inversion of VCM (i.e., $\mathbf{T}_{k-1}^{-1}$) which is assumed to be Hermitian in Proposition 2, in the sequel we shall discuss how to update $\mathbf{T}_k^{-1}$ (in order to make the next step of response control feasible) and how to

Algorithm 1: OPARC Algorithm.

1: give the initial weight vector $\mathbf{w}_0 = \mathbf{a}(\theta_0)$ and set $\mathbf{T}_0 = \mathbf{I}$, prescribe the direction θ_k and the corresponding desired level ρ_k, $k = 1, 2, \ldots$
2: **for** $k = 1, 2, \ldots,$ **do**
3: calculate $\gamma_{k,\star}$ from (26) and obtain $\mathbf{v}_k$ from (14)
4: update $\mathbf{w}_k$ as $\mathbf{w}_k = \mathbf{w}_{k-1} + \gamma_{k,\star}\mathbf{v}_k$
5: update $\mathbf{T}_k^{-1}$ as $\mathbf{T}_k^{-1} = \mathbf{T}_{k-1}^{-1} + \gamma_{k,\star}\mathbf{v}_k\mathbf{v}_k^{\mathrm{H}}/\xi_c$
6: **end for**
7: output $\mathbf{w}_k$ directly

guarantee the Hermitian property. To address these two problems, we first assume that $\mathbf{T}_{k-1}$ is Hermitian and the optimal $\gamma_{k,\star}$ has been obtained with the aid of Proposition 2. Then, from (12) we have

$$-\beta_{k,\star}/\left(1+\beta_{k,\star}\xi_k\right) = \gamma_{k,\star}/\xi_c \tag{30}$$

where $\beta_{k,\star} = \Psi_k^{-1}(\gamma_{k,\star})$ denotes the INR corresponding to $\gamma_{k,\star}$ in the kth step. Obviously, the combination of (10) and (30) yields

$$\mathbf{T}_k^{-1} = \mathbf{T}_{k-1}^{-1} + \frac{\gamma_{k,\star}\mathbf{v}_k\mathbf{v}_k^{\mathrm{H}}}{\xi_c}. \tag{31}$$

Therefore, $\mathbf{T}_k^{-1}$ can be calculated out straightforwardly (without the calculation of $\mathbf{T}_k$ and its inversion), once the optimal $\gamma_{k,\star}$ obtained.

To further explore the Hermitian property of $\mathbf{T}_k$, let us revisit Proposition 2 and get

$$\frac{\gamma_{k,\star}}{\xi_c} = -\frac{\left(\|\mathbf{c}_\gamma\|_2 \pm R_\gamma\right)\chi}{\|\mathbf{c}_\gamma\|_2\mathbf{H}_k(2,2)} \in \mathbb{R} \tag{32}$$

which is a real-valued number. Thus, it is known that $\mathbf{T}_k$ is Hermitian as long as $\mathbf{T}_{k-1}$ is Hermitian. Accordingly, it can be readily concluded that if we set $\mathbf{T}_0 = \mathbf{I}$, then $\mathbf{T}_i$ is Hermitian for $i = 1, 2, \ldots, k$.

Now, it is seen that the response levels can be successively adjusted by assigning virtual interferences. Therefore, we can utilize the above update procedures iteratively to fulfill the prescribed response control requirement. Note that in each step of our array response control, only the response level of the current angle θ_k can be precisely adjusted, and the responses of the previously-controlled angles may have some perturbations. This also implies that the index k can be even greater than $N-1$. Finally, the proposed OPARC method is summarized in Algorithm 1.

III. Some Properties of OPARC

In the previous section, we have shown that the response level at a certain direction can be optimally and flexibly adjusted by assigning a virtual interference. Instead of determining β_k (i.e., the INR of the virtue interference assigned in the kth step), an alternative parameter γ_k, mapping of β_k, is chosen to facilitate the algorithm derivation. However, since INR has a physical meaning and is always a non-negative value in a real data case, it is worth examining the direct relationship between the response level and β_k. To do so, in this section we continue the analysis on the OPARC scheme, mainly focus on the selection of INR β_k rather than its mapping γ_k.

A. Geometrical Distribution of β_k

As shown in (12), γ_k is a mapping of β_k, and β_k can be expressed with respect to γ_k as

$$\beta_k = -\gamma_k/\left(\xi_c + \gamma_k\xi_k\right) = \Psi_k^{-1}(\gamma_k) \tag{33}$$

where $\Psi_k^{-1}(\cdot)$ is the inverse function of $\Psi_k(\cdot)$ in (12). Thus, β_k can be calculated once γ_k is available. For the trajectory of β_k when the array response level ρ_k is satisfied at angle θ_k, let us recall Proposition 1 and express γ_k as

$$\gamma_k = \mathbf{c}_\gamma(1) + j\mathbf{c}_\gamma(2) + R_\gamma e^{j\varphi} \tag{34}$$

where $\mathbf{c}_\gamma$ and R_γ are the center and the radius of the circle given in Proposition 1, φ can be any real-valued number. Substituting (34) into (33), one gets

$$\beta_k = \left(p_1 + p_2 e^{j\varphi}\right)/\left(q_1 + q_2 e^{j\varphi}\right) \tag{35}$$

where p_l and q_l ($l = 1, 2$) are complex numbers satisfying

$$p_1 = -\mathbf{c}_\gamma(1) - j\mathbf{c}_\gamma(2), \qquad p_2 = -R_\gamma \tag{36a}$$

$$q_1 = \xi_c + \left(\mathbf{c}_\gamma(1) + j\mathbf{c}_\gamma(2)\right)\xi_k, \; q_2 = R_\gamma\xi_k. \tag{36b}$$

With some calculation, it is not difficult to have the following proposition.

Proposition 3: The trajectory of $[\Re(\beta_k)\ \Im(\beta_k)]^{\mathrm{T}}$ with β_k satisfying (35) is a circle $\mathbb{C}_\beta$ with the center

$$\mathbf{c}_\beta = \left[\xi_0/(|\xi_c|^2 - \xi_0\xi_k),\, 0\right]^{\mathrm{T}} \tag{37}$$

and the radius

$$R_\beta = |\xi_c|/\left[\sqrt{\rho_k}\cdot\left||\xi_c|^2 - \xi_0\xi_k\right|\right] \tag{38}$$

i.e.,

$$\beta_k = \mathbf{c}_\beta(1) + j\mathbf{c}_\beta(2) + R_\beta e^{j\phi} \tag{39}$$

where ϕ can be any real-valued number.

Similar to γ_k, all the β_k on the above circle can be used to precisely adjust the response level at θ_k to its desired level ρ_k. An interesting difference with γ_k is that the calculations of $\mathbf{c}_\beta$ and R_β do not require the knowledge of $\mathbf{w}_{k-1}$. This implies that all β_k's (including the optimal one later) can be obtained without knowing any weight vectors. On the contrary, the determination of γ_k relies on the availability of the previous weight vector $\mathbf{w}_{k-1}$.

In addition, Proposition 3 implies that the center of the trajectory of $[\Re(\beta_k)\ \Im(\beta_k)]^{\mathrm{T}}$ is located on the real axis, and is independent of the desired level ρ_k.

B. Determination of the Optimal β_k

Among all the valid β_k for the control of the array response level ρ_k at θ_k, the optimal one is the one that maximizes the array gain. Therefore, the following constrained optimization

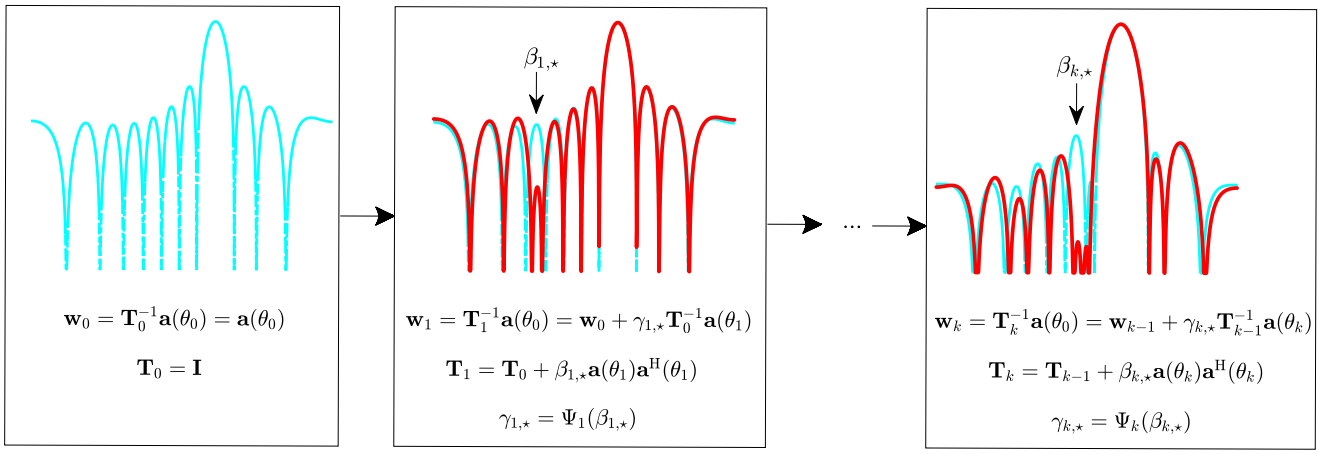

Fig. 2. Illustration of the proposed OPARC algorithm.

problem can be formulated to select the optimal β_k:

$$\underset{\beta_k}{\text{maximize}} \quad G_k = |\mathbf{w}_k^{\mathrm{H}}\mathbf{a}(\theta_0)|^2/|\mathbf{w}_k^{\mathrm{H}}\mathbf{T}_k\mathbf{w}_k| \tag{40a}$$

$$\text{subject to} \quad L(\theta_k,\theta_0) = \rho_k \tag{40b}$$

$$\mathbf{w}_k = \mathbf{w}_{k-1} + \Psi_k(\beta_k)\mathbf{T}_{k-1}^{-1}\mathbf{a}(\theta_k) \tag{40c}$$

where the parameter γ_k has been replaced in (40c) by $\Psi_k(\beta_k)$. Clearly, the above optimization problem (40) is equivalent to problem (21). Therefore, the optimal solution (denoted as $\beta_{k,\star}$) of (40) can be readily obtained by utilizing the mapping as

$$\beta_{k,\star} = \Psi_k^{-1}(\gamma_{k,\star}). \tag{41}$$

Combining the result of $\gamma_{k,\star}$ in (26) with some calculation, we can derive Proposition 4 below.

Proposition 4: The optimal solution of (40) is given by

$$\beta_{k,\star} = \begin{cases} \beta_{k,r}, & \text{if } -1/\xi_k > \xi_0/\left(|\xi_c|^2 - \xi_0\xi_k\right) \\ \beta_{k,l}, & \text{otherwise} \end{cases} \tag{42}$$

where $\beta_{k,r}$ and $\beta_{k,l}$ are the intersections of circle $\mathbb{C}_\beta$ and the real axis $\Im(\cdot) = 0$:

$$\beta_{k,r} = R_\beta + \xi_0/\left(|\xi_c|^2 - \xi_0\xi_k\right) \tag{43}$$

$$\beta_{k,l} = -R_\beta + \xi_0/\left(|\xi_c|^2 - \xi_0\xi_k\right). \tag{44}$$

It is not hard to see from (42) that the optimal $\beta_{k,\star}$ is a real-valued number, while the valid β_k in Proposition 3 for the array response control may be complex valued. However, as mentioned earlier, the physical meaning of β_k is the INR as it is used in (8) and it cannot be negative. From (42)–(44), the solved optimal $\beta_{k,\star}$ may be negative, which might be because there is no assumption of the used VCM $\mathbf{T}_{k-1}$ being non-negative definite. This will be studied together with the update of the VCM below. On the other hand, if $\mathbf{T}_{k-1}$ is Hermitian, then $\mathbf{T}_k = \mathbf{T}_{k-1} + \beta_{k,\star}\mathbf{a}(\theta_k)\mathbf{a}^{\mathrm{H}}(\theta_k)$ is also Hermitian, since $\beta_{k,\star}$ is real. This is consistent with the inference obtained in the paragraph below Eqn. (32). Finally, it is obvious that the optimal β_k in (42) does not depend on the knowledge of the weight vectors in the previous steps.

Algorithm 2: OPARC Algorithm (an Equivalent Variant).

1: give $\mathbf{a}(\theta_0)$ and set $\mathbf{T}_0 = \mathbf{I}$, specify the direction θ_k and the corresponding desired level ρ_k with $k = 1, 2, \ldots$
2: **for** $k = 1, 2, \ldots,$ **do**
3: calculate $\beta_{k,\star}$ from (42)
4: update $\mathbf{T}_k$ as $\mathbf{T}_k = \mathbf{T}_{k-1} + \beta_{k,\star}\mathbf{a}(\theta_k)\mathbf{a}^{\mathrm{H}}(\theta_k)$
5: **end for**
6: calculate $\mathbf{w}_k = \mathbf{T}_k^{-1}\mathbf{a}(\theta_0)$

Once the optimal β_k has been obtained, we can express the VCM at the current stage as

$$\mathbf{T}_k = \mathbf{T}_{k-1} + \beta_{k,\star}\mathbf{a}(\theta_k)\mathbf{a}^{\mathrm{H}}(\theta_k). \tag{45}$$

Since $\mathbf{T}_0 = \mathbf{I}$ is taken as the initial VCM, by taking all the assigned virtual interferences into consideration, one can alternatively express $\mathbf{T}_k$ as

$$\mathbf{T}_k = \mathbf{I} + \mathbf{A}_k\mathbf{\Sigma}_k\mathbf{A}_k^{\mathrm{H}} \tag{46}$$

where $\mathbf{A}_k \triangleq [\mathbf{a}(\theta_1), \ldots, \mathbf{a}(\theta_k)]$ and $\mathbf{\Sigma}_k$ is a diagonal matrix containing all β's of virtual interferences, i.e.,

$$\mathbf{\Sigma}_k = \mathrm{Diag}\left([\beta_{1,\star}, \beta_{2,\star}, \ldots, \beta_{k,\star}]\right). \tag{47}$$

Accordingly, we have $\mathbf{w}_k = \mathbf{T}_k^{-1}\mathbf{a}(\theta_0)$. To make it clear, the variant of the OPARC method is summarized in Algorithm 2. Note that the calculation of intermediate weight vectors is avoided, due to the fact that neither the calculation of $\beta_{k,\star}$ nor $\mathbf{T}_k$ relies on weight vectors. Therefore, the procedure of array response control is simplified. To have an intuitive understanding, a schematic diagram of OPARC is presented in Fig. 2, where the equations of weight vector updating are also incorporated.

Before proceeding, it is interesting to provide a deep insight and a geometrical perspective on the relationship between γ_k and β_k. It is not hard to see that the condition $-1/\xi_k > \xi_0/\left(|\xi_c|^2 - \xi_0\xi_k\right)$ in (42) is equivalent to the condition $\zeta > 0$ in (26), if and only if $\rho_k\xi_0 < \xi_k$. It implies that the conditions for selecting $\beta_{k,\star}$ between $\beta_{k,l}$ and $\beta_{k,r}$ and selecting $\gamma_{k,\star}$ between $\gamma_{k,a}$ and $\gamma_{k,b}$ may be different and are the same

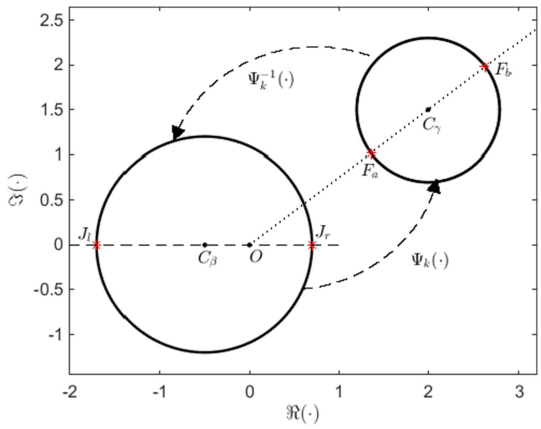

Fig. 3. Illustration of the mapping $\Psi_k(\cdot)$.

under a certain condition, i.e., $\rho_k\xi_0 < \xi_k$. Thus, we have

$$\begin{cases} \gamma_{k,a} = \Psi_k(\beta_{k,r}), \gamma_{k,b} = \Psi_k(\beta_{k,l}), & \text{if } \rho_k\xi_0 < \xi_k \\ \gamma_{k,a} = \Psi_k(\beta_{k,l}), \gamma_{k,b} = \Psi_k(\beta_{k,r}), & \text{otherwise.} \end{cases} \tag{48}$$

To have an intuitive perspective on $\Psi_k(\cdot)$, a geometrical illustration is given in Fig. 3, where J_r, J_l, F_a and F_b stand for the points $[\Re(\beta_{k,r})\ \Im(\beta_{k,r})]^{\mathrm{T}}$, $[\Re(\beta_{k,l})\ \Im(\beta_{k,l})]^{\mathrm{T}}$, $[\Re(\gamma_{k,a})\ \Im(\gamma_{k,a})]^{\mathrm{T}}$ and $[\Re(\gamma_{k,b})\ \Im(\gamma_{k,b})]^{\mathrm{T}}$, respectively.

C. Positive Definite Virtual Covariance Matrices

Firstly, the following conclusion, which simplifies the selection of $\beta_{k,\star}$, can be obtained.

Proposition 5: If $\mathbf{T}_{k-1} \in \mathbb{S}_{++}^N$, we have

$$\beta_{k,\star} = \beta_{k,r} = (|\xi_c| - \sqrt{\rho_k}\xi_0)/[\sqrt{\rho_k}(\xi_0\xi_k - |\xi_c|^2)]. \tag{49}$$

Furthermore, if $\mathbf{T}_{k-1} \in \mathbb{S}_{++}^N$, then $\mathbf{T}_k \in \mathbb{S}_{++}^N$ if and only if $\rho_k < \xi_k^2/|\xi_c|^2$.

Proof: See Appendix C. ■

Similar to the argument in the paragraph below Eqn. (20), $\xi_k^2/|\xi_c|^2$ is in general greater than 1 and it is assumed $\rho_k \leq 1$. Thus, we have $\rho_k < \xi_k^2/|\xi_c|^2$. As a consequence, in each step of weight vector update, we have $\mathbf{T}_k \in \mathbb{S}_{++}^N$ and $\beta_{k,\star} = \beta_{k,r}$, as long as $\mathbf{T}_{k-1} \in \mathbb{S}_{++}^N$. Since in our algorithm $\mathbf{T}_0 = \mathbf{I}$ is taken as the initial VCM, we have $\mathbf{T}_k \in \mathbb{S}_{++}^N$ and $\beta_{k,\star} = \beta_{k,r}$.

Proposition 6: If $\mathbf{T}_{k-1} \in \mathbb{S}_{++}^N$, then

$$\beta_{k,\star} \geq 0 \Leftrightarrow |\xi_c| \geq \sqrt{\rho_k}\xi_0 \tag{50a}$$

$$\beta_{k,\star} < 0 \Leftrightarrow |\xi_c| < \sqrt{\rho_k}\xi_0. \tag{50b}$$

Proof: From (75) in the proof of Proposition 5 in Appendix C, we have $\xi_0\xi_k - |\xi_c|^2 > 0$ provided that $\mathbf{T}_{k-1} \in \mathbb{S}_{++}^N$. Then, from (49), the proof of (50) is completed. ■

Substituting the definitions of ξ_c and ξ_0 into (50) and using $\mathbf{w}_{k-1} = \mathbf{T}_{k-1}^{-1}\mathbf{a}(\theta_0)$, we have

$$\beta_{k,\star} \geq 0 \Leftrightarrow \rho_k \leq \left|\mathbf{w}_{k-1}^{\mathrm{H}}\mathbf{a}(\theta_k)\right|^2 / \left|\mathbf{w}_{k-1}^{\mathrm{H}}\mathbf{a}(\theta_0)\right|^2 \tag{51a}$$

$$\beta_{k,\star} < 0 \Leftrightarrow \rho_k > \left|\mathbf{w}_{k-1}^{\mathrm{H}}\mathbf{a}(\theta_k)\right|^2 / \left|\mathbf{w}_{k-1}^{\mathrm{H}}\mathbf{a}(\theta_0)\right|^2. \tag{51b}$$

Notice that $\left|\mathbf{w}_{k-1}^{\mathrm{H}}\mathbf{a}(\theta_k)\right|^2 / \left|\mathbf{w}_{k-1}^{\mathrm{H}}\mathbf{a}(\theta_0)\right|^2$ above represents the normalized response at θ_k, of the previous weight vector $\mathbf{w}_{k-1}$. Clearly, (51) shows that the resultant $\beta_{k,\star}$ is non-negative if the desired level ρ_k is lower than the response level at θ_k of the previous weight vector $\mathbf{w}_{k-1}$. Otherwise, a negative $\beta_{k,\star}$ is obtained if it is required to elevate the previous response level of θ_k. We can see that the negative $\beta_{k,\star}$ is still meaningful in our discussion of array response control using virtual interferences, although it cannot occur in a real data covariance matrix with real interferences.

In addition to the above two propositions, the following result can be obtained.

Proposition 7: If $\mathbf{T}_{k-1} \in \mathbb{S}_{++}^N$, then problem (40) has the same optimal solution as that of the following one

$$\underset{\beta_k}{\text{maximize}} \quad \frac{|\mathbf{w}_k^{\mathrm{H}}\mathbf{a}(\theta_0)|^2}{\mathbf{w}_k^{\mathrm{H}}\mathbf{T}_{k-1}\mathbf{w}_k} \tag{52a}$$

$$\text{subject to} \quad L(\theta_k, \theta_0) = \rho_k \tag{52b}$$

$$\mathbf{w}_k = \mathbf{w}_{k-1} + \Psi_k(\beta_k)\mathbf{v}_k. \tag{52c}$$

Proof: See Appendix D. ■

Interestingly, from Proposition 7, it is known that under the same constraints (i.e., (40b) and (40c)), the optimal β_k to (40) also maximizes the previous array gain, in which only $\mathbf{T}_{k-1}$ (but not $\mathbf{T}_k$) is taken into consideration.

For instance, consider the case when $\mathbf{T}_{k-1}$ is a real normalized noise-plus-interference covariance matrix (i.e., $\mathbf{T}_{k-1}$ is calculated from real data that contains both noise and interference), and one applies the OPARC scheme to realize a specific array response control task in (52b) by assigning a virtual interference at θ_k. Then, it is seen from Proposition 7 that the optimal $\beta_{k,\star}$ of problem (40) also maximizes the real output SINR (not taking the virtual interference into consideration) of beamformer. This property will be further exploited in the companion paper [20] to design an adaptive beamformer with specific constraint.

IV. Comparison With A^{2}RC

In the above sections, the optimal values of γ_k and β_k of the virtual interference assigned in the kth step are specified. Meanwhile, useful conclusions are obtained and two versions of OPARC are described. In this section, comparisons will be carried out to elaborate the differences between the recent A^{2}RC algorithm [15] and the above OPARC algorithm from two perspectives.

A. Comparison on the Formula Updating

In the A^{2}RC method, the weight vector is updated as

$$\mathbf{w}_k = \mathbf{w}_{k-1} + \mu_k\mathbf{a}(\theta_k) \tag{53}$$

where μ_k is the hyperparameter to be optimized. To minimize the deviation between the resultant responses of adjacent two steps, and meanwhile, avoid the computationally inefficient global search, μ_k is empirically selected in [15] as $\mu_{k,a}$, which is the solution to the following problem:

$$\underset{\mu_k}{\text{minimize}} \quad |\mu_k| \tag{54a}$$

$$\text{subject to} \quad \left[\Re(\mu_k)\ \Im(\mu_k)\right]^{\mathrm{T}} \in \mathbb{C}_\mu \tag{54b}$$

where $\mathbb{C}_\mu$ is the following circle:

$$\mathbb{C}_\mu = \left\{ [\Re(\mu_k)\ \Im(\mu_k)]^{\mathrm{T}} \middle| \left\| [\Re(\mu_k)\ \Im(\mu_k)]^{\mathrm{T}} - \mathbf{c}_\mu \right\|_2 = R_\mu \right\}$$

with the center

$$\mathbf{c}_\mu = \frac{1}{\mathbf{Q}_k(2,2)} \begin{bmatrix} -\Re\left[\mathbf{Q}_k(1,2)\right] \\ \Im\left[\mathbf{Q}_k(1,2)\right] \end{bmatrix} \tag{55}$$

and the radius

$$R_\mu = \sqrt{-\det(\mathbf{Q}_k)} \big/ |\mathbf{Q}_k(2,2)| \tag{56}$$

where the matrix $\mathbf{Q}_k$ satisfies

$$\mathbf{Q}_k = [\mathbf{w}_{k-1}\ \mathbf{a}(\theta_k)]^{\mathrm{H}} \big(\mathbf{a}(\theta_k)\mathbf{a}^{\mathrm{H}}(\theta_k) - \rho_k \mathbf{a}(\theta_0)\mathbf{a}^{\mathrm{H}}(\theta_0)\big)[\mathbf{w}_{k-1}\ \mathbf{a}(\theta_k)].$$

Note that such an empirical selection may not perform well under all circumstances. As a matter of fact, this scheme may even lead to severe pattern distortion, as we will show later in simulations in Section V.

In the OPARC algorithm, the weight vector is updated via (21c). It is seen that, different from the A^{2}RC algorithm, a scaling of $\mathbf{T}_{k-1}^{-1}\mathbf{a}(\theta_k)$ is added to $\mathbf{w}_{k-1}$, and $\gamma_k \mathbf{T}_{k-1}^{-1}\mathbf{a}(\theta_k)$ makes the resultant $\mathbf{w}_k$ be an optimal weight vector.

Additionally, in the proposed OPARC algorithm, we optimize the parameter γ_k by maximizing the array gain when the preassigned response level is satisfied.

To have a similar weight form with A^{2}RC, it is shown in Appendix E that we can reformulate (21c) as

$$\begin{aligned} \mathbf{w}_k &= \mathbf{w}_{k-1} + \gamma_k \mathbf{A}(\theta_k, \ldots, \theta_1)\mathbf{d}_k \\ &= \mathbf{w}_{k-1} + \gamma_k \mathbf{a}(\theta_k) + \gamma_k \mathbf{A}(\theta_{k-1}, \ldots, \theta_1)\bar{\mathbf{d}}_k \end{aligned} \tag{57}$$

where $\mathbf{A}(\theta_k, \ldots, \theta_1) \triangleq [\mathbf{a}(\theta_k), \ldots, \mathbf{a}(\theta_1)]$, with θ_i $(1 \le i \le k-1)$ denoting the angles of interferences that assigned previously, $\mathbf{d}_k$ is a $k \times 1$ vector with its first element 1, $\bar{\mathbf{d}}_k$ is a $(k-1) \times 1$ vector obtained by removing the first element from $\mathbf{d}_k$. From (57), it is observed that the added component to the previous weight vector $\mathbf{w}_{k-1}$ in $\mathbf{w}_k$ is a linear combination of the steering vectors of all interferences (including both the current $\mathbf{a}(\theta_k)$ and the previous $\mathbf{a}(\theta_1), \ldots, \mathbf{a}(\theta_{k-1})$). On the contrary, in the A^{2}RC algorithm, the added component is a scaling of the steering vector of the single interference to be assigned (i.e., $\mathbf{a}(\theta_k)$). Furthermore, we can obtain the following corollary of Proposition 2, which describes a similarity between A^{2}RC and OPARC.

Corollary 1: In the first step of weight update (i.e, $\mathbf{w}_0 = \mathbf{a}(\theta_0)$, $\mathbf{T}_0 = \mathbf{I}$), if $\rho_1 \le \|\mathbf{a}(\theta_1)\|_2^2 / \|\mathbf{a}(\theta_0)\|_2^2$, then $\mu_{1,\star} = \gamma_{1,\star}$, otherwise, $\mu_{1,\star} = \gamma_{1,\times}$, where $\gamma_{1,\times} = \{\gamma_{1,a}, \gamma_{1,b}\} \setminus \gamma_{1,\star}$.

Proof: See Appendix F. ■

From Corollary 1, it is known that in the first step of the weight vector update, A^{2}RC will lead to the same result as OPARC, provided that $\rho_1 \le \|\mathbf{a}(\theta_1)\|_2^2 / \|\mathbf{a}(\theta_0)\|_2^2$. Otherwise, the inferior parameter $\gamma_{1,\times}$ (in the sense of array gain) will be adopted by A^{2}RC. For the other steps of the weight vector update, i.e., $k > 1$, the proposed OPARC algorithm takes the optimal parameter and thus obtains a better performance than that of A^{2}RC. Consequently, we know that OPARC always performs at least as good as A^{2}RC, for a given array response control task.

B. Comparison on INRs of Virtual Interferences

We next compare the INRs of virtual interferences to show an essential difference between A^{2}RC and OPARC. To begin with, we express the weight vector of A^{2}RC in the kth step as

$$\begin{aligned} \mathbf{w}_k &= \mathbf{a}(\theta_0) + \mu_1 \mathbf{a}(\theta_1) + \ldots + \mu_k \mathbf{a}(\theta_k) \\ &= \mathbf{a}(\theta_0) + \mathbf{A}_k \mathbf{b}_k \end{aligned} \tag{58}$$

where $\mathbf{b}_k \triangleq [\mu_1, \mu_2, \ldots, \mu_k]^{\mathrm{T}}$. Note from the above that the update of the weight vector $\mathbf{w}_k$ in A^{2}RC does not depend on any VCM and no VCM update is needed. However, in order to compare the INRs, we need to associate it to a VCM that may be implicit/virtual. To do so, we rewrite the weight vector as

$$\begin{aligned} \mathbf{w}_k &= \breve{\mathbf{T}}_k^{-1}\mathbf{a}(\theta_0) \\ &= \mathbf{a}(\theta_0) - \mathbf{A}_k \left(\mathbf{I} + \breve{\mathbf{\Sigma}}_k \mathbf{A}_k^{\mathrm{H}} \mathbf{A}_k\right)^{-1} \breve{\mathbf{\Sigma}}_k \mathbf{A}_k^{\mathrm{H}} \mathbf{a}(\theta_0) \end{aligned} \tag{59}$$

where $\breve{\mathbf{T}}_k = \mathbf{I} + \mathbf{A}_k \breve{\mathbf{\Sigma}}_k \mathbf{A}_k^{\mathrm{H}}$ denotes a VCM, $\breve{\mathbf{\Sigma}}_k = \mathrm{Diag}([\breve{\beta}_{k,1}, \breve{\beta}_{k,2}, \ldots, \breve{\beta}_{k,k}])$ specifies the INR of the interference at θ_i $(i = 1, \ldots, k)$ when completing the current kth step of the weight vector update.

Note that no interference was assigned at the current θ_k in the previous $k-1$ steps of the response control. It is shown from Appendix G that in the kth step of the weight update of the A^{2}RC algorithm, the INR of the virtual interference assigned at θ_k is

$$\breve{\beta}_{k,k} = -\frac{\mu_k}{\mathbf{a}^{\mathrm{H}}(\theta_k)\breve{\mathbf{w}}_{k-1} + \mu_k \|\mathbf{a}(\theta_k)\|_2^2}. \tag{60}$$

In addition, $k-1$ new interferences are additively assigned at directions $\theta_1, \ldots, \theta_{k-1}$ of A^{2}RC to the previous $(k-1)$th step. Denote the INRs of these new interferences assigned at θ_i in the kth step of the weight update as $\breve{\Delta}_{k,i}$ $(1 \le i \le k-1)$. Clearly they satisfy

$$\breve{\Delta}_{k,i} = \breve{\beta}_{k,i} - \breve{\beta}_{k-1,i}. \tag{61}$$

It can be further derived (see Appendix G) that

$$\breve{\Delta}_{k,i} = \frac{\mu_k \mathbf{a}^{\mathrm{H}}(\theta_i)\mathbf{a}(\theta_k)\breve{\beta}_{k-1,i}^2}{\mu_i - \mu_k \mathbf{a}^{\mathrm{H}}(\theta_i)\mathbf{a}(\theta_k)\breve{\beta}_{k-1,i}}. \tag{62}$$

Generally speaking, in the kth step of A^{2}RC, the INRs of the newly-assigned interferences (including both $\breve{\beta}_{k,k}$ and $\breve{\Delta}_{k,i}$ $(1 \le i \le k-1)$) are complex-valued numbers. This is a difference between A^{2}RC and OPARC. Moreover, the above analysis shows that there are $k-1$ additional interferences assigned to the previously controlled angles (i.e., $\theta_1, \ldots, \theta_{k-1}$) in the kth step of A^{2}RC, while in OPARC only a single interference is assigned (at θ_k). Since our aim is to control the array response level at θ_k, the newly-assigned virtual interferences at $\theta_1, \ldots, \theta_{k-1}$ actually bring undesirable array response variations at these adjusted angles. According to the above notations, the VCM of A^{2}RC satisfies implicitly:

$$\breve{\mathbf{T}}_k = \breve{\mathbf{T}}_{k-1} + \mathbf{A}_k \mathrm{Diag}([\breve{\Delta}_{k,1}, \ldots, \breve{\Delta}_{k,k-1}, \breve{\beta}_{k,k}])\mathbf{A}_k^{\mathrm{H}} \tag{63}$$

TABLE I
ELEMENT LOCATIONS AND ELEMENT PATTERNS OF THE NONUNIFORM LINEAR ARRAY (USED IN THE FIRST AND THE SECOND EXAMPLES)

n	x_n	$g_n(\theta)$	n	x_n	$g_n(\theta)$
1	0.00	$1.00\cos(1.00\theta)$	7	3.05	$1.02\cos(1.00\theta)$
2	0.45	$0.98\cos(0.85\theta)$	8	3.65	$1.08\cos(0.90\theta)$
3	1.00	$1.05\cos(0.98\theta)$	9	4.03	$0.96\cos(0.75\theta)$
4	1.55	$1.10\cos(0.70\theta)$	10	4.60	$1.09\cos(0.92\theta)$
5	2.10	$0.90\cos(0.85\theta)$	11	5.00	$1.02\cos(0.80\theta)$
6	2.60	$0.93\cos(0.69\theta)$			

which is different from that of OPARC in (45).

To summarize, the main differences between the proposed OPARC algorithm and the existing A^{2}RC algorithm include:

- Different formulas of the weight update are employed in OPARC and A^{2}RC.
- The resultant weight of OPARC can be guaranteed to be an optimal beamformer, while A^{2}RC method does not.
- The array gain is introduced to the parameter optimization of OPARC, while A^{2}RC is not.
- The update of VCM is necessary for OPARC, while A^{2}RC is free of this procedure although its VCM is implicitly updated by (63).
- Two different strategies of virtual interference assigning are adopted in these two approaches. The INRs of OPARC are always real, but they may not be in A^{2}RC.

V. SIMULATION RESULTS

We next present some simulations to verify the effectiveness of our proposed OPARC. To validate the superiority of OPARC, we also test another precise array response control (PARC) scheme, in which we adopt the following non-optimal parameter intentionally:

$$\gamma_k = \gamma_{k,\times} \triangleq \{\gamma_{k,a}, \gamma_{k,b}\} \setminus \gamma_{k,\star} \tag{64}$$

and use the same remaining procedure as OPARC. Denote $\beta_{k,\times} = \Psi_k^{-1}(\gamma_{k,\times})$. Note that $\gamma_{1,\times}$ is the same as that in Corollary 1. Clearly, PARC can precisely control array response level as well, while its parameter γ_k is not optimally selected as in OPARC. Besides OPARC and PARC, the A^{2}RC algorithm in [15] is also compared. We set $\omega = 6\pi \times 10^8$ rad/s, which corresponds to a wavelength $\lambda = 2\pi c/\omega = 1$ m with the light speed c. Unless otherwise specified, we consider a 11-element non-uniformly spaced linear array with nonisotropic elements. Both the element locations x_n and the element patterns $g_n(\theta)$ are listed in Table I, from which the $\tau_n(\theta)$ in (2) can be specified as $\tau_n(\theta) = x_n \sin(\theta)/c$. Additionally, we take the quiescent weight vector $\mathbf{a}(\theta_0)$ as the initial weight and fix the beam axis at $\theta_0 = 20^\circ$ except otherwise specified.

An ideal criterion of array response control is to achieve the desired level at θ_k while keeping the responses at any other directions unchanged. However, such a criterion cannot be achieved, since the array response is a continuous function. In fact, a good array response result would bring less changes on the previously-controlled angles. According to this criterion, we introduce two cost functions to measure the performances of different methods. The first one is defined as

$$D_k \triangleq |L_k(\theta_{k-1}, \theta_0) - L_{k-1}(\theta_{k-1}, \theta_0)| \tag{65}$$

where $L_k(\theta, \theta_0)$ represents the resultant response after finishing the k-th step of weight update. Since the response level at θ_{k-1} has been adjusted in the $(k-1)$th step as its desired level ρ_{k-1}, one can rewrite D_k as $D_k = |L_k(\theta_{k-1}, \theta_0) - \rho_{k-1}|$. It can be seen that D_k measures the level difference between the resulting response and the desired one at the previously-controlled angle θ_{k-1}, after the k-th step of array response control. The second cost function is defined as

$$J_k \triangleq \frac{1}{k-1} \sum_{i=1}^{k-1} \big| L_k(\theta_i, \theta_0) - \rho_i \big| \tag{66}$$

which measures the average difference between the resulting response and the desired one at the previously-controlled angles θ_i's, $i = 1, \ldots, k-1$, after the k-th step of array response control. Moreover, J_k is effective on measuring the level difference between the resulting response and the desired one, even if the initial or previous responses are unqualified. Clearly, both D_k and J_k are expected to be small if the array response level is well adjusted. In addition, we should set $k \geq 2$ in the measurements of D_k and J_k. For $k = 2$, one can readily obtain that $D_k = J_k$, and only the metric D_k is considered in this case. Besides D_k and J_k above, we also test the obtained array gains of different methods, and consider pattern variation and pattern distortion for performance comparison.

A. Pattern Variation

In the first example, we test the performances of different approaches for sidelobe response control. For convenience, we carry out two steps of the array response control algorithms and denote the two adjusted angles as θ_1 and θ_2, respectively. More specifically, the normalized responses at $\theta_1 = -45^\circ$ and $\theta_2 = -5^\circ$ are expected to be successively adjusted to $\rho_1 = -40$ dB and $\rho_2 = -30$ dB.

In the first step of response control, we can figure out that $\mathbf{c}_\gamma = [-0.1704, -0.0315]^{\mathrm{T}}$, $d = -8.5231 - j1.5766$, $\gamma_{1,a} = -0.1559 - j0.0288$ and $\gamma_{1,b} = -0.1849 - j0.0342$. On this basis, we obtain that $\zeta = 1 > 0$ and hence choose $\gamma_{1,\star} = \gamma_{1,a}$ for OPARC and select $\gamma_{1,\times} = \gamma_{1,b}$ for PARC, according to (26) and (64), respectively. Additionally, it can be figured out that $\mathbf{c}_\beta = [-0.1488, 0]^{\mathrm{T}}$ and $R_\beta = 1.7171$. We adopt $\beta_{1,\star} = \beta_{1,r} = 1.5683$ for OPARC (so that the resulting array gain is maximized and the resulting weight vector is optimal) and take $\beta_{1,\times} = \beta_{1,l} = -1.8659$ for PARC.

For A^{2}RC, it is found that $\mu_1 = \gamma_{1,\star} = -0.1559 - j0.0288$, which coincides with the result of Corollary 1. As predicted, one also obtains that $\breve{\beta}_{1,1} = \beta_{1,\star} = 1.5683$. Fig. 4(a) illustrates the resultant response patterns of different schemes after controlling the response level of θ_1. As we can see, all these three approaches are capable of precisely controlling the array response levels as expected. Notice also that the result of A^{2}RC is exactly the same as that of OPARC, which can obtain an optimal beamformer when there exists an interference (with INR $\beta_{1,\star}$) at θ_1.

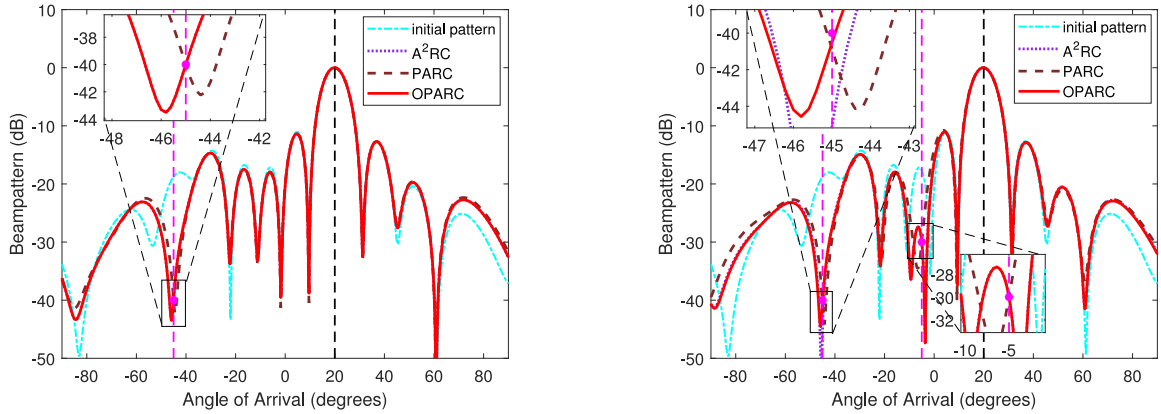

(a) Synthesized patterns at the 1st step

(b) Synthesized patterns at the 2nd step

Fig. 4. Resultant pattern comparison (the first example).

TABLE II
OBTAINED PARAMETER COMPARISON (THE FIRST EXAMPLE)

	A^{2}RC	PARC	OPARC
D_2(dB)	5.05	0.86	0.51
G_1(dB)	10.0482	10.0331	10.0482
G_2(dB)	10.0026	9.9653	10.0074

In the second step, with the same manner we found out that $\gamma_{2,\star} = -0.0685 - j0.0399$, $\beta_{2,\star} = 0.2504$, $\gamma_{2,\times} = -0.1148 - j0.0695$, $\beta_{2,\times} = -0.4277$ and $\mu_2 = -0.0674 - j0.0393$. Fig. 4(b) depicts the results of different methods after controlling the response level of the second angle θ_2. It is seen that all methods can adjust $L(\theta_2, \theta_0)$ to ρ_2. For the proposed OPARC scheme, it can be checked that $\beta_{k,r}$ is the ultimate selection of $\beta_{k,\star}$ $(k = 1, 2)$. In fact, this is consistent with the conclusion of Proposition 5. One can see that both $\beta_{1,\star}$ and $\beta_{2,\star}$ are positive in this case. This coincides with the theoretical prediction of Proposition 6, since it is required to lower the response levels in either step. After the second step of array response control, the resulting beamformer of OPARC is an optimal one that maximizes the output SINR when two interferences exist at θ_1 and θ_2 with INRs $\beta_{1,\star}$ and $\beta_{2,\star}$, respectively.

To further examine the performance, we evaluate D_2 (or equivalently J_2) as defined earlier and list their measurements in Table II. It is observed that the proposed OPARC scheme minimizes D_2 among the three methods. From Table II and Fig. 4(b), it is found that A^{2}RC causes serious perturbation (about 5 dB) at the previous point θ_1. In fact, besides the virtual interference assigned at θ_2, another one is also assigned at the previously adjusted direction (i.e., θ_1), for the existing A^{2}RC algorithm. We can calculate that $\breve{\beta}_{2,2} = 0.2465 + j0.0001$ and $\breve{\Delta}_{2,1} = -0.4120 + j2.5879$ (INR of the additional interference assigned at θ_1 in the second step of response control). Notice that both $\breve{\beta}_{2,2}$ and $\breve{\Delta}_{2,1}$ are complex numbers, which is different from that of OPARC. Finally, we have listed the obtained array gains of these approaches at both steps in Table II. Clearly, it is seen that OPARC outperforms the other two methods.

Since the metric D_2 depends on the desired level at θ_2 (i.e., ρ_2), we vary ρ_2 from -50 dB to -20 dB and recalculate D_2 with the other settings unchanged. Fig. 5 plots the curves of D_2 versus ρ_2. It can be clearly observed that the proposed OPARC algorithm performs the best on D_2. Recalling the definition of D_k, Fig. 5 implies that OPARC brings a less perturbation to θ_1 compared to its desired level. The existing A^{2}RC causes a large deviation to the response level at θ_1 as displayed in Fig. 5.

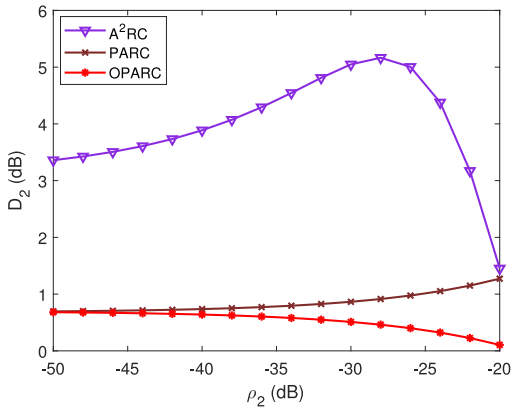

Fig. 5. Curves of D_2 versus ρ_2 (the first example).

B. Pattern Distortion

In this part, we shall further show the advantages of the OPARC. For convenience, we set θ_1 and its desired level ρ_1 the same as the first example, and then conduct the second step of the response control by taking $\theta_2 = 23^\circ$ and $\rho_2 = 0$ dB. Notice that θ_2 is in the mainlobe region in this case, and it is required to elevate the response level there.

Clearly, the obtained parameters of the second step are renewed for all methods tested, while the results of the first step keep unaltered compared to the previous example. Here, it can be obtained with the A^{2}RC algorithm that $\mu_2 = -0.5931 + j0.8040$, $\breve{\beta}_{2,2} = -0.3923 - j0.4011$ and $\breve{\Delta}_{2,1} = -1.8001 + j0.0334$. For the PARC algorithm, we obtain $\gamma_{2,\times} = -0.7108 + j0.7171$ and $\beta_{2,\times} = -0.8522$. While for OPARC, its parameter satisfies $\gamma_{2,\star} = \gamma_{2,b} = 0.8352 - j0.8438$ and $\beta_{2,\star} = \beta_{2,r} = -0.0577$. It is worth noting that we have selected γ_b, which is different from that at Step 1 (where γ_a is selected), to

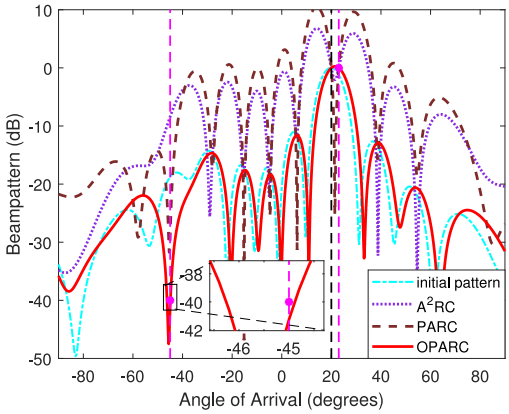

Fig. 6. Comparison of synthesized patterns at the 2nd step of the 2nd example.

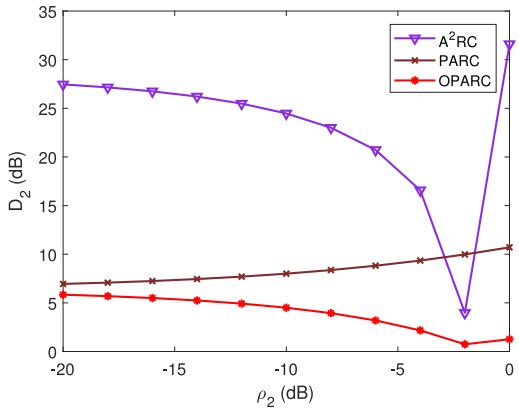

Fig. 7. Curves of D_2 versus ρ_2 (the second example).

TABLE III
OBTAINED PARAMETER COMPARISON (THE SECOND EXAMPLE)

	A^{2}RC	PARC	OPARC
D_2(dB)	31.6001	10.7083	1.2595
G_2(dB)	2.5060	0.7366	13.1370

obtain the final $\gamma_{2,\star}$. In fact, this flexible mechanism of parameter determination in OPARC enables us to avoid certain pattern distortion, which is inevitable in A^{2}RC or PARC. To see this clearer, we have depicted the synthesized patterns in Fig. 6. It can be found that all the response levels at θ_2 still meet the requirement as before. However, it shows clearly that the patterns of A^{2}RC and PARC are severely distorted. The obtained mainlobes are split and the resultant sidelobe levels are raised for both A^{2}RC and PARC. For the proposed OPARC, none of the above undesirable phenomena happens and a well-shaped pattern has been obtained. Notice that $\beta_{2,\star}$ is negative in this scenario. This is consistent with the conclusion of Proposition 6, since the response level needs to be lifted in this second step of response control. It should be emphasized that the resulting weight of OPARC is optimal on maximizing the output SINR if two interferences exist at θ_1 and θ_2 with INRs $\beta_{1,\star}$ and $\beta_{2,\star}$, respectively.

The details of D_2 and the obtained array gains have been specified in Table III, from which the merits of the proposed OPARC algorithm are clearly observed. Note that the array gain G_1 is not listed in Table III since it has been reported in Table II. Again, to further examine the performance, we vary ρ_2 from -20 dB to 0 dB, and depict the curve of D_2 versus ρ_2 in Fig. 7. As illustrated in this figure, A^{2}RC causes a great perturbation on θ_1 (i.e., high value of D_2). On the other hand, OPARC performs the best when measuring D_2.

C. Further Investigation With Randomized Array Configurations

To show that our algorithm behaves well not only under carefully chosen array configurations, we carry out the third example by randomly selecting the element number and positions, and taking the influence of mutual coupling into consideration as well. In this case, we consider a linear array with isotropic elements. The beam axis is taken as $\theta_0 = -10^\circ$. We pre-assign ten angles and their corresponding desired levels, see Table IV for details. To present a fair comparison, we carry out Monte Carlo simulation by taking the realization number as 1000, and then depict the resulting D_k, J_k and G_k in an average sense. In each realization, the element number N is randomly selected as a positive integer from 8 to 16, so that the number of controlled points may be either less or greater than N. The element space between two adjacent sensors is distributed uniformly in the range $[0.4\lambda, 0.6\lambda]$. The mutual coupling matrix (denoted as $\mathbf{Z} \in \mathbb{C}^{N\times N}$) is complex symmetry with unit elements on diagonal. The amplitudes of other entries of $\mathbf{Z}$ are fixed as 0.1, and their phases are distributed uniformly in the range $[0, 2\pi)$. In addition, the PARC algorithm is not considered in this example, since it always performs worse than OPARC as shown in the previous two examples.

TABLE IV
SETTINGS OF θ_k AND ρ_k

k	θ_k	ρ_k(dB)	k	θ_k	ρ_k(dB)
1	-80°	-40	6	-60°	-30
2	-13°	-0.5	7	-45°	-30
3	10°	-20	8	-30°	-40
4	-7°	0	9	40°	-40
5	20°	-40	10	78°	-35

Fig. 9 illustrates several intermediate results of one realization with $N = 8$. In particular, Fig. 8(b) and Fig. 8(c) present the synthesized patterns at the 9th and the 10th steps, respectively. Note from Fig. 8(b) and Fig. 8(c) that the response level of θ_9 or θ_{10} can still be adjusted precisely for both algorithms, although the corresponding iteration index k has become greater than the element number N and the resulting beampatterns of A^{2}RC have been distorted.

To present the superiority of OPARC, the curves of average D_k, J_k and G_k have also been depicted in Fig. 9, with the increase of the iteration index k. For each iteration step, Fig. 9 shows that the proposed OPARC results smaller values on D_k and J_k and obtains a higher array gain G_k, when comparing to the A^{2}RC algorithm. Therefore, the proposed OPARC algorithm

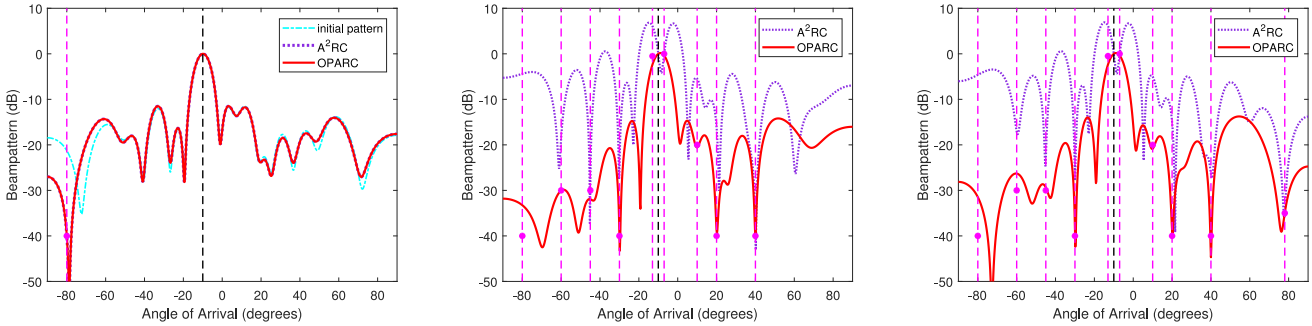

(a) Synthesized patterns at the 1st step (b) Synthesized patterns at the 9th step (c) Synthesized patterns at the 10th step

Fig. 8. One realization of resultant patterns (the third example).

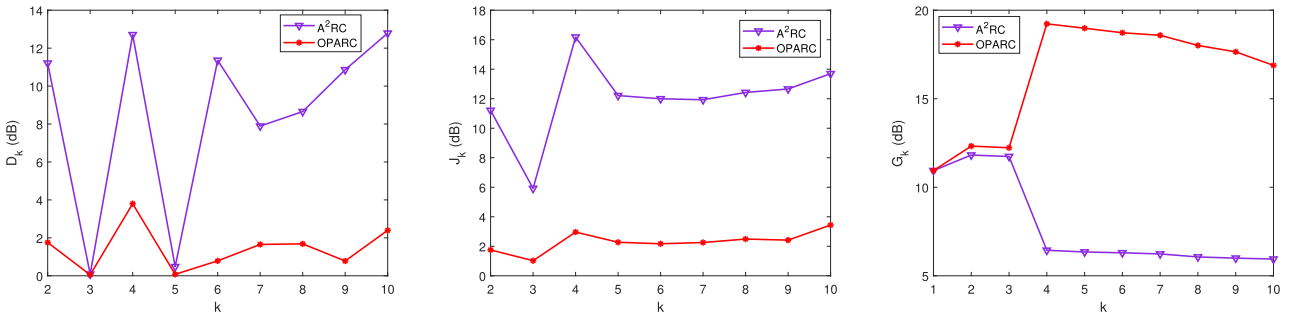

(a) Curves of average D_k versus iteration index k (b) Curves of average J_k versus iteration index k (c) Curves of average G_k versus iteration index k

Fig. 9. Performance comparison (the third example).

performs well not only under the circumstances of carefully chosen array configurations.

VI. Conclusion

In this paper, a novel algorithm of optimal and precise array response control (OPARC) has been proposed. This algorithm origins from the adaptive array theory and the change rule of the optimal weight vector, when adding interferences one by one, has been found. Then, the parameter selection mechanism has been carried out to maximize the array gain with the constraint that the response level at one direction is precisely adjusted. Some properties of OPARC have been presented and OPARC is compared in details with A^{2}RC. Finally, simulation results have been shown to illustrate the effectiveness of the proposed OPARC method. Based on the fundamentals developed in this paper, a further extension of OPARC to multi-point array response control and its applications to, for example, pattern synthesis, multi-constraint adaptive beamforming and quiescent pattern control will be considered in [20].

Appendix A
Proof of Proposition 1

For the sake of clarity, the subscript k will be omitted in the sequel. To solve the equation (16), we take the eigenvalue decomposition of $\mathbf{H}$, i.e., $\mathbf{H}=\mathbf{U}\mathbf{\Lambda}\mathbf{U}^{\mathrm{H}}$, where $\mathbf{U}$ is an unitary matrix, $\mathbf{\Lambda}=\mathrm{Diag}([\lambda_1,\lambda_2])$ with λ_1 and λ_2 are eigenvalues of $\mathbf{H}$. Let us define $\mathbf{y}\triangleq\mathbf{U}^{\mathrm{H}}\mathbf{z}$, then (16) can be equivalently expressed as $\mathbf{y}^{\mathrm{H}}\mathbf{\Lambda}\mathbf{y}=0$, and further $\lambda_1|\mathbf{y}(1)|^2+\lambda_2|\mathbf{y}(2)|^2=0$.

Before proceeding, it can be found that $\det(\mathbf{H})=-\rho_k\left|\mathbf{w}_{k-1}^{\mathrm{H}}\mathbf{a}(\theta_0)\mathbf{v}_k^{\mathrm{H}}\mathbf{a}(\theta_k)-\mathbf{w}_{k-1}^{\mathrm{H}}\mathbf{a}(\theta_k)\mathbf{v}_k^{\mathrm{H}}\mathbf{a}(\theta_0)\right|^2\le 0$. On this basis, by utilizing the fact that $\lambda_1\lambda_2=\det(\mathbf{H})\le 0$, we learn that $\lambda_1|\mathbf{y}(1)|^2+\lambda_2|\mathbf{y}(2)|^2=0$ can be solved. Let us express $\mathbf{U}$ as $\mathbf{U}=\left[\begin{smallmatrix}u_{11} & u_{12}\\ u_{21} & u_{22}\end{smallmatrix}\right]$, then we have

$$\begin{aligned}
&\lambda_1|\mathbf{y}(1)|^2+\lambda_2|\mathbf{y}(2)|^2\\
&=\lambda_1|u_{11}^*+u_{21}^*\gamma|^2+\lambda_2|u_{12}^*+u_{22}^*\gamma|^2\\
&=\mathbf{H}(1,1)+2\Re\left[\mathbf{H}(1,2)\right]\cdot\Re(\gamma)-2\Im\left[\mathbf{H}(1,2)\right]\cdot\Im(\gamma)\\
&\quad+\mathbf{H}(2,2)\left[\Re^2(\gamma)+\Im^2(\gamma)\right]\\
&=0
\end{aligned}\tag{67}$$

where we have utilized the fact that

$$\mathbf{H}(1,1)=\lambda_1|u_{11}|^2+\lambda_2|u_{12}|^2 \tag{68a}$$

$$\mathbf{H}(1,2)=\lambda_1u_{21}^*u_{11}+\lambda_2u_{22}^*u_{12} \tag{68b}$$

$$\mathbf{H}(2,1)=\lambda_1u_{11}^*u_{21}+\lambda_2u_{12}^*u_{22} \tag{68c}$$

$$\mathbf{H}(2,2)=\lambda_1|u_{21}|^2+\lambda_2|u_{22}|^2. \tag{68d}$$

From (67), it is known that if $\mathbf{H}(2,2)=0$, we have $\Re\left[\mathbf{H}(1,2)\right]\cdot\Re(\gamma)-\Im\left[\mathbf{H}(1,2)\right]\cdot\Im(\gamma)=-\mathbf{H}(1,1)/2$. Otherwise, if $\mathbf{H}(2,2)\neq 0$, (67) can be expressed as

$$\left(\Re(\gamma)+\frac{\Re\left[\mathbf{H}(1,2)\right]}{\mathbf{H}(2,2)}\right)^2+\left(\Im(\gamma)-\frac{\Im\left[\mathbf{H}(1,2)\right]}{\mathbf{H}(2,2)}\right)^2=-\frac{\det(\mathbf{H})}{\mathbf{H}^2(2,2)}$$

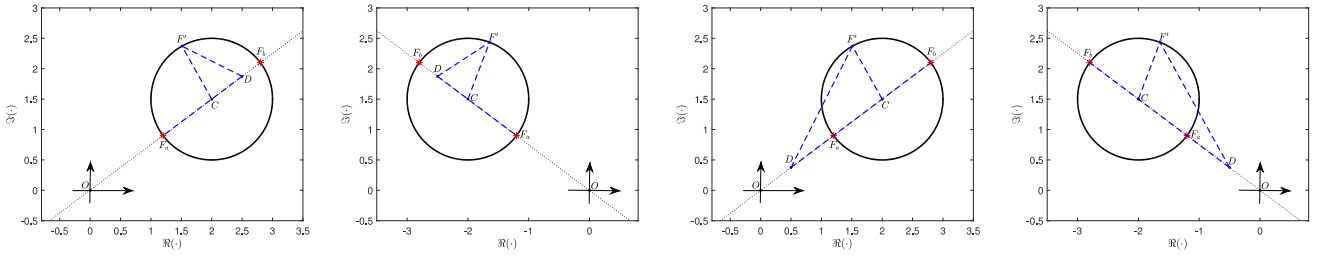

(a) $\Re(d) > \mathbf{c}_\gamma(1) \geq 0$ (b) $\Re(d) < \mathbf{c}_\gamma(1) < 0$ (c) $\mathbf{c}_\gamma(1) \geq 0$ and $\Re(d) < \mathbf{c}_\gamma(1)$ (d) $\mathbf{c}_\gamma(1) < 0$ and $\Re(d) > \mathbf{c}_\gamma(1)$

Fig. 10. Geometrical illustration of different cases when maximizing array gain.

which implies that the trajectory of $[\Re(\gamma)\ \Im(\gamma)]^{\mathrm{T}}$ is a circle with the center $\mathbf{c}_\gamma$ in (18) and the radius R_γ in (19). This completes the proof of Proposition 1.

Appendix B
Proof of Proposition 2

Since $\mathbf{T}_{k-1}$ is assumed to be Hermitian, both ξ_0 and ξ_k are real-valued and one also gets $\widetilde{\xi}_c = \xi_c^*$. According to (17), we have

$$\mathbf{H}_k(1,2) = \mathbf{w}_{k-1}^{\mathrm{H}}[\mathbf{a}(\theta_k)\mathbf{a}^{\mathrm{H}}(\theta_k) - \rho_k \mathbf{a}(\theta_0)\mathbf{a}^{\mathrm{H}}(\theta_0)]\mathbf{v}_k = \chi \xi_c^*$$

where $\chi = \xi_k - \rho_k \xi_0 \in \mathbb{R}$. From (18), we have

$$\mathbf{c}_\gamma(1) + j\mathbf{c}_\gamma(2) = -\chi \xi_c / \mathbf{H}_k(2,2). \tag{69}$$

Thus,

$$\gamma_{k,a} = -\frac{(\|\mathbf{c}_\gamma\|_2 - R_\gamma)\,\chi \xi_c}{\|\mathbf{c}_\gamma\|_2 \mathbf{H}_k(2,2)},\ \gamma_{k,b} = -\frac{(\|\mathbf{c}_\gamma\|_2 + R_\gamma)\,\chi \xi_c}{\|\mathbf{c}_\gamma\|_2 \mathbf{H}_k(2,2)}.$$

From (69) and both χ and $\mathbf{H}_k(2,2)$ are real, we have

$$\mathbf{c}_\gamma(2)/\mathbf{c}_\gamma(1) = \Im(\xi_c)/\Re(\xi_c). \tag{70}$$

For the array gain G_k in (23) we have

$$\begin{aligned} G_k &= |\xi_c^*| \cdot |\xi_0/\xi_c^* + \gamma_k| = |\xi_c^*| \cdot |\gamma_k - d| \\ &= |\xi_c^*| \cdot \left\| \left[\Re(\gamma_k)\ \Im(\gamma_k)\right]^{\mathrm{T}} - \left[\Re(d)\ \Im(d)\right]^{\mathrm{T}} \right\|_2 \end{aligned} \tag{71}$$

where $d = -\xi_0/\xi_c^*$. Also,

$$\Im(d)/\Re(d) = \Im(\xi_c)/\Re(\xi_c) = \mathbf{c}_\gamma(2)/\mathbf{c}_\gamma(1). \tag{72}$$

This shows that the origin $\mathbf{O}$, the center $\mathbf{c}_\gamma$ and $D = [\Re(d)\ \Im(d)]^{\mathrm{T}}$ are co-linear on the plane as shown in Fig. 10. Note that in Fig. 10 we have denoted C as the center of the circle. From (71) it can be observed that G_k is a scaling of the Euclidean distance between D and a point $F = [\Re(\gamma_k), \Im(\gamma_k)]^{\mathrm{T}}$ located on the circle $\mathbb{C}_\gamma$. From this observation, the optimal solution to (21) can thus be obtained in a geometrical approach below.

Without loss of generality, we first assume that $\Re(d) \neq \mathbf{c}_\gamma(1)$, otherwise, all γ_k on circle $\mathbb{C}_k$ will have the same G_k. In the case of $\Re(d) > \mathbf{c}_\gamma(1) \geq 0$ or $\Re(d) < \mathbf{c}_\gamma(1) < 0$, it can be derived that $\gamma_{k,\star} = \gamma_{k,a}$, i.e., when $F = F_a$, G_k is maximized. In fact, these two cases can be geometrically illustrated by Fig. 10(a) and Fig. 10(b), respectively.

Similarly, in the case of $\mathbf{c}_\gamma(1) \geq 0$, $\Re(d) < \mathbf{c}_\gamma(1)$ (as shown in Fig. 10(c)), or $\mathbf{c}_\gamma(1) < 0$, $\Re(d) > \mathbf{c}_\gamma(1)$ (as shown in Fig. 10(d)), the two points O and D are located on the same sides (right or left) of C. As a result, $\gamma_{k,\star} = \gamma_{k,b}$, i.e., when $F = F_b$, G_k is maximized in these two cases.

In summary, it can be concluded that if $\zeta > 0$, $\gamma_{k,\star} = \gamma_{k,a}$, otherwise, $\gamma_{k,\star} = \gamma_{k,b}$, where ζ has been defined in (27). This completes the proof.

Appendix C
Proof of Proposition 5

It is easy to see that $-1/\xi_k > \xi_0/\left(|\xi_c|^2 - \xi_0\xi_k\right)$ in (42) is actually equivalent to

$$(|\xi_c|^2 - \xi_0\xi_k)\xi_k < 0. \tag{73}$$

When $\mathbf{T}_{k-1} \in \mathbb{S}_{++}^N$, we have $\mathbf{T}_{k-1}^{-1} \in \mathbb{S}_{++}^N$. Thus, from (24b)

$$\xi_k > 0. \tag{74}$$

Let the Cholesky decomposition of $\mathbf{T}_{k-1}^{-1}$ be $\mathbf{T}_{k-1}^{-1} = \mathbf{\Xi}\mathbf{\Xi}^{\mathrm{H}}$, where $\mathbf{\Xi}$ is an invertible matrix. If $\mathbf{a}(\theta_0) \neq \varrho \mathbf{a}(\theta_k)$ for $\forall \varrho \in \mathbb{C}$ that always holds in array antenna theory, we have $\mathbf{\Xi}^{\mathrm{H}}\mathbf{a}(\theta_0) \neq \varrho \mathbf{\Xi}^{\mathrm{H}}\mathbf{a}(\theta_k)$ for $\forall \varrho \in \mathbb{C}$. Then, from the Cauchy-Schwarz inequity we have

$$\begin{aligned} |\xi_c|^2 - \xi_0\xi_k &= \left|(\mathbf{\Xi}^{\mathrm{H}}\mathbf{a}(\theta_k))^{\mathrm{H}}(\mathbf{\Xi}^{\mathrm{H}}\mathbf{a}(\theta_0))\right|^2 \\ &\quad - \left\|\mathbf{\Xi}^{\mathrm{H}}\mathbf{a}(\theta_0)\right\|_2^2 \cdot \left\|\mathbf{\Xi}^{\mathrm{H}}\mathbf{a}(\theta_k)\right\|_2^2 < 0. \end{aligned} \tag{75}$$

Hence, from Proposition 4, we have $\beta_{k,\star} = \beta_{k,r}$.

From (38), (43) and the fact that $\beta_{k,\star} = \beta_{k,r}$, we have

$$\beta_{k,\star} = \frac{|\xi_c| - \sqrt{\rho_k}\xi_0}{\sqrt{\rho_k}(\xi_0\xi_k - |\xi_c|^2)}. \tag{76}$$

This completes the proof of (49).

Furthermore, if $\mathbf{T}_{k-1} \in \mathbb{S}_{++}^N$, one learns from $\mathbf{T}_k = \mathbf{T}_{k-1} + \beta_{k,\star}\mathbf{a}(\theta_k)\mathbf{a}^{\mathrm{H}}(\theta_k)$ that

$$\mathbf{T}_k \in \mathbb{S}_{++}^N \Leftrightarrow \mathbf{T}_{k-1} + \beta_{k,\star}\mathbf{a}(\theta_k)\mathbf{a}^{\mathrm{H}}(\theta_k) \in \mathbb{S}_{++}^N \tag{77a}$$

$$\Leftrightarrow \mathbf{I} + \beta_{k,\star}\mathbf{T}_{k-1}^{-1/2}\mathbf{a}(\theta_k)\mathbf{a}^{\mathrm{H}}(\theta_k)\mathbf{T}_{k-1}^{-1/2} \in \mathbb{S}_{++}^N \tag{77b}$$

$$\Leftrightarrow 1 + \beta_{k,\star}\mathbf{a}^{\mathrm{H}}(\theta_k)\mathbf{T}_{k-1}^{-1}\mathbf{a}(\theta_k) > 0 \tag{77c}$$

$$\Leftrightarrow \beta_{k,\star} > -1/\xi_k \tag{77d}$$

$$\Leftrightarrow \frac{|\xi_c|\xi_k - \sqrt{\rho_k}|\xi_c|^2}{\sqrt{\rho_k}(\xi_0\xi_k - |\xi_c|^2)\xi_k} > 0 \tag{77e}$$

$$\Leftrightarrow \rho_k < \xi_k^2/|\xi_c|^2. \tag{77f}$$

This completes the proof of Proposition 5.

APPENDIX D
PROOF OF PROPOSITION 7

From the update procedure of weight vector, one gets

$$\begin{aligned}\mathbf{w}_k &= \mathbf{w}_{k-1} + \gamma_k \mathbf{v}_k \\ &= \mathbf{T}_{k-1}^{-1}\mathbf{a}(\theta_0) - \beta_k \xi_c \mathbf{T}_{k-1}^{-1}\mathbf{a}(\theta_k)/(1+\beta_k\xi_k). \end{aligned} \tag{78}$$

Then we can obtain $\mathbf{a}^{\mathrm{H}}(\theta_0)\mathbf{w}_k = \xi_0 - \beta_k|\xi_c|^2/(1+\beta_k\xi_k)$ and

$$|\mathbf{w}_k^{\mathrm{H}}\mathbf{a}(\theta_0)|^2 = |(\xi_0\xi_k - |\xi_c|^2)\beta_k + \xi_0|^2 / |1+\beta_k\xi_k|^2. \tag{79}$$

On the other hand, from (78) we have $\mathbf{w}_k^{\mathrm{H}}\mathbf{T}_{k-1} = \mathbf{a}^{\mathrm{H}}(\theta_0) - \beta_k^*\xi_c^*\mathbf{a}^{\mathrm{H}}(\theta_k)/(1+\beta_k^*\xi_k)$ and further get

$$\begin{aligned}\mathbf{w}_k^{\mathrm{H}}\mathbf{T}_{k-1}\mathbf{w}_k =\ & \left(\mathbf{a}^{\mathrm{H}}(\theta_0) - \beta_k^*\xi_c^*\mathbf{a}^{\mathrm{H}}(\theta_k)/(1+\beta_k^*\xi_k)\right) \\ & \cdot \left(\mathbf{T}_{k-1}^{-1}\mathbf{a}(\theta_0) - \beta_k\xi_c\mathbf{T}_{k-1}^{-1}\mathbf{a}(\theta_k)/(1+\beta_k\xi_k)\right) \\ =\ & \frac{(\xi_0\xi_k - |\xi_c|^2)\xi_k|\beta_k + \frac{1}{\xi_k}|^2 + \frac{|\xi_c|^2}{\xi_k}}{|1+\beta_k\xi_k|^2}. \end{aligned} \tag{80}$$

Combining (79) and (80), we get

$$\frac{|\mathbf{w}_k^{\mathrm{H}}\mathbf{a}(\theta_0)|^2}{\mathbf{w}_k^{\mathrm{H}}\mathbf{T}_{k-1}\mathbf{w}_k} = \frac{\left(\frac{\xi_0\xi_k - |\xi_c|^2}{\xi_k}\right)\cdot R_\beta^2}{\left|\beta_k + \frac{1}{\xi_k}\right|^2 + \frac{|\xi_c|^2}{(\xi_0\xi_k - |\xi_c|^2)\xi_k^2}} \tag{81}$$

where we have utilized the fact that $\xi_0\xi_k - |\xi_c|^2 > 0$ (see (75) when $\mathbf{T}_{k-1}^{-1} \in \mathbb{S}_{++}^N$) and $\left|\beta_k + \frac{\xi_0}{\xi_0\xi_k - |\xi_c|^2}\right| = R_\beta$. Obviously, the maximization of $|\mathbf{w}_k^{\mathrm{H}}\mathbf{a}(\theta_0)|^2/(\mathbf{w}_k^{\mathrm{H}}\mathbf{T}_{k-1}\mathbf{w}_k)$ is equivalent to minimizing $\left|\beta_k + \frac{1}{\xi_k}\right|$. Define

$$\mathbf{f} \triangleq \begin{bmatrix} -1/\xi_k & 0 \end{bmatrix}^{\mathrm{T}} \tag{82}$$

then we can reformulate problem (52) as

$$\underset{\beta_k}{\text{minimize}} \quad \|[\Re(\beta_k)\ \Im(\beta_k)]^{\mathrm{T}} - \mathbf{f}\|_2 \tag{83a}$$

$$\text{subject to} \quad [\Re(\beta_k)\ \Im(\beta_k)]^{\mathrm{T}} \in \mathbb{C}_\beta. \tag{83b}$$

On the other hand, substituting the constraint (40c) into G_k and recalling the conclusion of Proposition 3, the array gain satisfies

$$G_k = \left|\mathbf{a}^{\mathrm{H}}(\theta_0)\mathbf{T}_k^{-1}\mathbf{a}(\theta_0)\right| \tag{84a}$$

$$= \left|\xi_0 - \frac{\beta_k|\xi_c|^2}{1+\beta_k\xi_k}\right| \tag{84b}$$

$$= \left|\frac{\xi_0\xi_k - |\xi_c|^2}{\xi_k}\right| \cdot \left|\frac{\beta_k - \xi_0/\left(|\xi_c|^2 - \xi_0\xi_k\right)}{\beta_k - (-1/\xi_k)}\right| \tag{84c}$$

$$= \left|\frac{\xi_0\xi_k - |\xi_c|^2}{\xi_k}\right| \cdot \frac{\|[\Re(\beta_k)\ \Im(\beta_k)]^{\mathrm{T}} - \mathbf{c}_\beta\|_2}{\|[\Re(\beta_k)\ \Im(\beta_k)]^{\mathrm{T}} - \mathbf{f}\|_2} \tag{84d}$$

$$= \frac{\left|\left(\xi_0\xi_k - |\xi_c|^2\right)\cdot R_\beta/\xi_k\right|}{\|[\Re(\beta_k)\ \Im(\beta_k)]^{\mathrm{T}} - \mathbf{f}\|_2}. \tag{84e}$$

Note that (84a) comes from the intermediate result of (23), whereas (84d) is obtained from the result of Proposition 3. Since $\left|\left(\xi_0\xi_k - |\xi_c|^2\right)\cdot R_\beta/\xi_k\right|$ is a constant, from (84e), we can also reformulate problem (40) as (83).

Consequently, if $\mathbf{T}_{k-1} \in \mathbb{S}_{++}^N$, problem (40) has the same optimal solution as the problem (52). This completes the proof.

APPENDIX E
DERIVATION OF (57)

We first show

$$\mathbf{T}_{k-1}^{-1}\mathbf{a}(\theta_t) = \mathbf{A}(\theta_t, \theta_{k-1}, \ldots, \theta_1)\mathbf{d}_k(\theta_t),\ \forall \theta_t \in \mathbb{R} \tag{85}$$

where the first component of $\mathbf{d}_k(\theta_t)$ is 1.

We use induction to prove (85). When $k=1$, since $\mathbf{T}_0 = \mathbf{I}$, (85) is obvious, where $\mathbf{d}_1(\theta_t)$ degenerates to the scalar 1.

Suppose (85) is true when $k=p$, i.e.,

$$\mathbf{T}_{p-1}^{-1}\mathbf{a}(\theta_s) = \mathbf{A}(\theta_s, \theta_{p-1}, \ldots, \theta_1)\mathbf{d}_p(\theta_s),\ \forall \theta_s \in \mathbb{R} \tag{86}$$

where $\mathbf{d}_p(\theta_s)$ is a $p\times 1$ vector with its first entry 1.

When $k = p+1$, we want to show

$$\mathbf{T}_p^{-1}\mathbf{a}(\theta_r) = \mathbf{A}(\theta_r, \theta_p, \ldots, \theta_1)\mathbf{d}_{p+1}(\theta_r),\ \forall \theta_r \in \mathbb{R} \tag{87}$$

where $\mathbf{d}_{p+1}(\theta_r)$ is a $(p+1)\times 1$ vector with its first entry 1.

To see (87), one recalls (10) with $k=p$, and (86), and obtains (88) shown at the bottom of this page, where

$$\nu = -\beta_p\mathbf{a}^{\mathrm{H}}(\theta_p)\mathbf{T}_{p-1}^{-1}\mathbf{a}(\theta_r)/[1+\beta_p\mathbf{a}^{\mathrm{H}}(\theta_p)\mathbf{T}_{p-1}^{-1}\mathbf{a}(\theta_p)] \tag{89}$$

$\mathbf{d}_{p+1}(\theta_r)$ is a $(p+1)\times 1$ vector as shown in (90) shown at the bottom of this page, where $\mathbf{d}_p(\theta_r)_i$ stands for the ith element of $\mathbf{d}_p(\theta_r)$.

Then, (57) can be seen by substituting (85) with $\theta_t = \theta_k$ into (21c).

APPENDIX F
PROOF OF COROLLARY 1

In the first step of the weight vector update in the OPARC, we have $\mathbb{C}_\gamma = \mathbb{C}_\mu$ due to the fact that $\mathbf{T}_0 = \mathbf{I}$ and hence $\mathbf{H}_1 = \mathbf{Q}_1$. Therefore, one gets $\mu_{1,\star} = \gamma_{1,a}$ since $[\Re(\gamma_{1,a})\ \Im(\gamma_{1,a})]^{\mathrm{T}}$ has the minimum module among the elements in the set $\mathbb{C}_\gamma$ as shown in Fig. 1.

$$\begin{aligned}\mathbf{T}_p^{-1}\mathbf{a}(\theta_r) = \mathbf{T}_{p-1}^{-1}\mathbf{a}(\theta_r) + \nu\mathbf{T}_{p-1}^{-1}\mathbf{a}(\theta_p) &= \mathbf{A}(\theta_r, \theta_{p-1}, \ldots, \theta_1)\mathbf{d}_p(\theta_r) + \nu\mathbf{A}(\theta_p, \theta_{p-1}, \ldots, \theta_1)\mathbf{d}_p(\theta_p) \\ &= \mathbf{A}(\theta_r, \theta_p, \ldots, \theta_1)\mathbf{d}_{p+1}(\theta_r),\ \forall \theta_r \in \mathbb{R} \end{aligned} \tag{88}$$

$$\mathbf{d}_{p+1}(\theta_r) = [\mathbf{d}_p(\theta_r)_1, 0, \mathbf{d}_p(\theta_r)_2, \ldots, \mathbf{d}_p(\theta_r)_p]^{\mathrm{T}} + \nu\,[0, \mathbf{d}_p(\theta_p)_p, \mathbf{d}_p(\theta_r)_{p-1}, \ldots, \mathbf{d}_p(\theta_r)_1]^{\mathrm{T}} \tag{90}$$

$$\mathbf{1} \oslash \operatorname{diag}(\breve{\boldsymbol{\Sigma}}_k) = -(\mathbf{A}_k^{\mathrm{H}} \breve{\mathbf{w}}_k) \oslash \mathbf{b}_k = -\begin{bmatrix} \mathbf{A}_{\mathbf{k-1}}^{\mathrm{H}} \breve{\mathbf{w}}_{\mathbf{k}} \\ \mathbf{a}^{\mathrm{H}}(\theta_k) \breve{\mathbf{w}}_k \end{bmatrix} \oslash \begin{bmatrix} \mathbf{b_{k-1}} \\ \mu_k \end{bmatrix} = -\begin{bmatrix} (\mathbf{A}_{k-1}^{\mathrm{H}} \breve{\mathbf{w}}_{k-1}) \oslash \mathbf{b}_{k-1} + (\mu_k \mathbf{A}_{k-1}^{\mathrm{H}} \mathbf{a}(\theta_k)) \oslash \mathbf{b}_{k-1} \\ \mathbf{a}^{\mathrm{H}}(\theta_k) \breve{\mathbf{w}}_{k-1}/\mu_k + \|\mathbf{a}(\theta_k)\|_2^2 \end{bmatrix}$$

$$= \begin{bmatrix} \mathbf{1} \oslash \operatorname{diag}(\breve{\boldsymbol{\Sigma}}_{\mathbf{k-1}}) - (\mu_{\mathbf{k}} \mathbf{A}_{\mathbf{k-1}}^{\mathrm{H}} \mathbf{a}(\theta_{\mathbf{k}})) \oslash \mathbf{b_{k-1}} \\ -\mathbf{a}^{\mathrm{H}}(\theta_k) \breve{\mathbf{w}}_{k-1}/\mu_k - \|\mathbf{a}(\theta_k)\|_2^2 \end{bmatrix} \tag{92}$$

On the other hand, substituting $\mathbf{v}_1 = \mathbf{a}(\theta_1)$ and $\mathbf{w}_0 = \mathbf{a}(\theta_0)$ into (17) yields $\mathbf{H}_1(1,2) = (\|\mathbf{a}(\theta_1)\|_2^2 - \rho_1 \|\mathbf{a}(\theta_0)\|_2^2) \cdot \mathbf{a}^{\mathrm{H}}(\theta_0)\mathbf{a}(\theta_1)$ and $\mathbf{H}_1(2,2) = \|\mathbf{a}(\theta_1)\|_2^4 - \rho_1 |\mathbf{a}^{\mathrm{H}}(\theta_1)\mathbf{a}(\theta_0)|^2$. Recalling (18), we obtain

$$\mathbf{c}_\gamma(1) = \frac{-\Re\left[\mathbf{a}^{\mathrm{H}}(\theta_0)\mathbf{a}(\theta_1)\right](\|\mathbf{a}(\theta_1)\|_2^2 - \rho_1 \|\mathbf{a}(\theta_0)\|_2^2)}{\|\mathbf{a}(\theta_1)\|_2^4 - \rho_1 |\mathbf{a}^{\mathrm{H}}(\theta_1)\mathbf{a}(\theta_0)|^2}.$$

Meanwhile, since $\mathbf{T}_0 = \mathbf{I}$, one obtains from (27) that $\zeta = \operatorname{sign}(\|\mathbf{a}(\theta_1)\|_2^2 - \rho_1 \|\mathbf{a}(\theta_0)\|_2^2)$. Finally, from (26), if $\rho_1 \leq \|\mathbf{a}(\theta_1)\|_2^2 / \|\mathbf{a}(\theta_0)\|_2^2$, we have $\gamma_{1,\star} = \gamma_{1,a}$, otherwise, we obtain $\gamma_{1,\star} = \gamma_{1,b}$. Recalling $\mu_{1,\star} = \gamma_{1,a}$, we complete the proof.

Appendix G
Proof of (60) and (62)

From the equivalence of (58) and (59), one gets $\mathbf{b}_k = -(\mathbf{I} + \breve{\boldsymbol{\Sigma}}_k \mathbf{A}_k^{\mathrm{H}} \mathbf{A}_k)^{-1} \breve{\boldsymbol{\Sigma}}_k \mathbf{A}_k^{\mathrm{H}} \mathbf{a}(\theta_0)$. Multiplying by $\mathbf{I} + \breve{\boldsymbol{\Sigma}}_k \mathbf{A}_k^{\mathrm{H}} \mathbf{A}_k$ to both sides from the left of this equality yields $\breve{\boldsymbol{\Sigma}}_k \mathbf{A}_k^{\mathrm{H}} (\mathbf{a}(\theta_0) + \mathbf{A}_k \mathbf{b}_k) = -\mathbf{b}_k$. Since $\breve{\boldsymbol{\Sigma}}_k$ is a diagonal matrix and $\breve{\mathbf{w}}_k = \mathbf{a}(\theta_0) + \mathbf{A}_k \mathbf{b}_k$, we obtain

$$\breve{\boldsymbol{\Sigma}}_k = \operatorname{Diag}\left(-\mathbf{b}_k \oslash (\mathbf{A}_k^{\mathrm{H}} \breve{\mathbf{w}}_k)\right). \tag{91}$$

Furthermore, as $\mathbf{w}_k = \mathbf{w}_{k-1} + \mu_k \mathbf{a}(\theta_k)$, $\mathbf{b}_k = [\mathbf{b}_{k-1}^{\mathrm{T}} \ \mu_k]^{\mathrm{T}}$ and $\mathbf{A}_k = [\mathbf{A}_{k-1} \ \mathbf{a}(\theta_k)]$, we can rewrite (91) as (92) shown at the top of this page. Consequently, the following formulation can be obtained:

$$\frac{1}{\breve{\beta}_{k,i}} = \begin{cases} \dfrac{1}{\breve{\beta}_{k-1,i}} - \dfrac{\mu_k \mathbf{a}^{\mathrm{H}}(\theta_i)\mathbf{a}(\theta_k)}{\mu_i}, & 1 \leq i \leq k-1 \\ -\dfrac{\mathbf{a}^{\mathrm{H}}(\theta_k)\breve{\mathbf{w}}_{k-1}}{\mu_k} - \|\mathbf{a}(\theta_k)\|_2^2, & i = k. \end{cases} \tag{93}$$

From (93), the powers of interferences can be clearly observed. After some calculation, either (60) or (62) can be derived. This completes the proof.

Acknowledgment

The authors would like to thank the editor and the anonymous reviewers for their valuable comments and suggestions.

References

[1] R. J. Mailous, *Phased Array Antenna Handbook*. Norwood, MA, USA: Artech House, 1994.
[2] C. L. Dolph, "A current distribution for broadside arrays which optimizes the relationship between beam width and side-lobe level," *Proc. IRE*, vol. 34, pp. 335–348, 1946.
[3] K. Chen, X. Yun, Z. He, and C. Han, "Synthesis of sparse planar arrays using modified real genetic algorithm," *IEEE Trans. Antennas Propag.*, vol. 55, no. 4, pp. 1067–1073, Apr. 2007.
[4] V. Murino, A. Trucco, and C. S. Regazzoni, "Synthesis of unequally spaced arrays by simulated annealing," *IEEE Trans. Signal Process.*, vol. 44, no. 1, pp. 119–122, Jan. 1996.
[5] D. W. Boeringer and D. H. Werner, "Particle swarm optimization versus genetic algorithms for phased array synthesis," *IEEE Trans. Antennas Propag.*, vol. 52, no. 3, pp. 771–779, Mar. 2004.
[6] C. A. Olen and R. T. Compton, "A numerical pattern synthesis algorithm for arrays," *IEEE Trans. Antennas Propag.*, vol. 38, no. 10, pp. 1666–1676, Oct. 1990.
[7] P. Y. Zhou and M. A. Ingram, "Pattern synthesis for arbitrary arrays using an adaptive array method," *IEEE Trans. Antennas Propag.*, vol. 47, no. 5, pp. 862–869, May 1999.
[8] H. Lebret and S. Boyd, "Antenna array pattern synthesis via convex optimization," *IEEE Trans. Signal Process.*, vol. 45, no. 3, pp. 526–532, Mar. 1997.
[9] W. Fan, V. Balakrishnan, P. Y. Zhou, J. J. Chen, R. Yang, and C. Frank, "Optimal array pattern synthesis using semidefinite programming," *IEEE Trans. Signal Process.*, vol. 51, no. 5, pp. 1172–1183, May 2003.
[10] B. Fuchs, "Application of convex relaxation to array synthesis problems," *IEEE Trans. Antennas Propag.*, vol. 62, no. 2, pp. 634–640, Feb. 2014.
[11] C. Y. Tseng and L. J. Griffiths, "A simple algorithm to achieve desired patterns for arbitrary arrays," *IEEE Trans. Signal Process.*, vol. 40, no. 11, pp. 2737–2746, Nov. 1992.
[12] W. Stutzman, "Sidelobe control of antenna patterns," *IEEE Trans. Antennas Propag.*, vol. AP-20, no. 1, pp. 102–104, Jan. 1972.
[13] J. C. Sureau and K. Keeping, "Sidelobe control in cylindrical arrays," *IEEE Trans. Antennas Propag.*, vol. AP-30, no. 5, pp. 1027–1031, Sep. 1982.
[14] T. B. Vu, "Sidelobe control in circular ring array," *IEEE Trans. Antennas Propag.*, vol. 41, no. 8, pp. 1143–1145, Aug. 1993.
[15] X. Zhang, Z. He, B. Liao, X. Zhang, Z. Cheng, and Y. Lu, "A^{2}RC: An accurate array response control algorithm for pattern synthesis," *IEEE Trans. Signal Process.*, vol. 65, no. 7, pp. 1810–1824, Apr. 2017.
[16] X. Zhang, Z. He, B. Liao, X. Zhang, and W. Peng, 'Pattern synthesis for arbitrary arrays via weight vector orthogonal decomposition," *IEEE Trans. Signal Process.*, vol. 66, no. 5, pp. 1286–1299, Mar. 2018.
[17] X. Zhang, Z. He, B. Liao, X. Zhang, and W. Peng, "Pattern synthesis with multipoint accurate array response control," *IEEE Trans. Antennas Propag.*, vol. 65, no. 8, pp. 4075–4088, Aug. 2017.
[18] H. K. Van Trees, *Optimum Array Processing*. New York, NY, USA: Wiley, 2002.
[19] L. Griffiths and K. Buckley, "Quiescent pattern control in linearly constrained adaptive arrays," *IEEE Trans. Acoust., Speech, Signal Process.*, vol. ASSP-35, no. 7, pp. 917–926, Jul. 1987.
[20] X. Zhang, Z. He, X.-G. Xia, B. Liao, X. Zhang, and Y. Yang, "OPARC: Optimal and precise array response control algorithm—Part II: Multipoints and applications," *IEEE Trans. Signal Process.*, vol. 67, no. 3, pp. 668–683, 2018.
[21] G. H. Golub and C. F. V. Loan, *Matrix Computations*. Baltimore, MD, USA: Johns Hopkins Univ. Press, 1996.

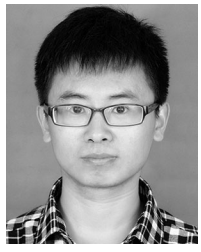

Xuejing Zhang (S'17) was born in Hebei, China. He received the B.S. degree in electrical engineering from Huaqiao University, Xiamen, China, in 2011, and the M.S. degree in signal and information processing from Xidian University, Xi'an, China, in 2014. He is currently working toward the Ph.D. degree in signal and information processing with the Department of Electronic Engineering, University of Electronic Science and Technology of China, Chengdu, China. Since November 2017, he has been a Visiting Student with the University of Delaware, Newark, DE, USA. From 2014 to 2015, he was a Research Engineer with the Allwinner Inc., Zhuhai, China, where he was engaged in algorithmic research. His research interests include array signal processing, optimization theory, and machine learning.

Zishu He (M'11) was born in Sichuan, China, in 1962. He received the B.S., M.S., and Ph.D. degrees in signal and information processing from the University of Electronic Science and Technology of China (UESTC), Chengdu, China, in 1984, 1988, and 2000, respectively.

He is currently a Professor of signal and information processing with the School of Electronic Engineering, UESTC. His current research interests are involved in array signal processing, digital beam forming, the theory on multiple-input multiple-output (MIMO) communication and MIMO radar, adaptive signal processing, and interference cancelation.

Xiang-Gen Xia (M'97–SM'00–F'09) received the B.S. degree in mathematics from Nanjing Normal University, Nanjing, China, in 1983, the M.S. degree in mathematics from Nankai University, Tianjin, China, in 1986, and the Ph.D. degree in electrical engineering from the University of Southern California, Los Angeles, CA, USA, in 1992.

From 1995 to 1996, he was a Senior/Research Staff Member with Hughes Research Laboratories, Malibu, CA, USA. In September 1996, he joined the Department of Electrical and Computer Engineering, University of Delaware, Newark, DE, USA, where he is currently the Charles Black Evans Professor. His current research interests include space-time coding, multiple-input multiple-output and orthogonal frequency division multiplexing systems, digital signal processing, and synthetic aperture radar and inverse synthetic aperture radar imaging. He is the author of the book *Modulated Coding for Intersymbol Interference Channels* (New York, NY, USA: Marcel Dekker, 2000).

Dr. Xia was the recipient of the National Science Foundation Faculty Early Career Development (CAREER) Program Award in 1997, the Office of Naval Research Young Investigator Award in 1998, and the Outstanding Overseas Young Investigator Award from the National Nature Science Foundation of China in 2001. He is currently serving and has served as an Associate Editor for numerous international journals including the IEEE WIRELESS COMMUNICATIONS LETTERS, the IEEE TRANSACTIONS ON SIGNAL PROCESSING, the IEEE TRANSACTIONS ON WIRELESS COMMUNICATIONS, the IEEE TRANSACTIONS ON MOBILE COMPUTING, and the IEEE TRANSACTIONS ON VEHICULAR TECHNOLOGY. He is a Technical Program Chair of the Signal Processing Symposium, Globecom 2007, Washington, DC, USA, and the General Co-Chair of the International Conference on Acoustics, Speech, and Signal Processing 2005, Philadelphia, PA, USA.

Bin Liao (S'09–M'13–SM'16) received the B.Eng. and M.Eng. degrees from Xidian University, Xi'an, China, in 2006 and 2009, respectively, and the Ph.D. degree from The University of Hong Kong, Hong Kong, in 2013, all in electronic engineering. From September 2013 to January 2014, he was a Research Assistant with the Department of Electrical and Electronic Engineering, The University of Hong Kong, where he was a Research Scientist from August 2016 to October 2016. He is currently an Associate Professor with the College of Information Engineering, Shenzhen University, Shenzhen, China. His research interests include sensor array processing, adaptive filtering, convex optimization, with applications to radar, navigation, and communications.

Dr. Liao is an Associate Editor for the IEEE TRANSACTIONS ON AEROSPACE AND ELECTRONIC SYSTEMS, *IET Signal Processing, Multidimensional Systems and Signal Processing*, and the IEEE ACCESS. He was the recipient of the Best Paper Award at the 21st International Conference on Digital Signal Processing in 2016 and the 22nd International Conference on Digital Signal Processing in 2017.

Xuepan Zhang was born in Hebei, China. He received the B.S. degree in electrical engineering from Xidian University, Xi'an, China, in 2010, and the Ph.D. degree from the National Laboratory of Radar Signal Processing, Xidian University, in 2015. He is currently a Principal Investigator with the Qian Xuesen Laboratory of Space Technology, Beijing, China. His research interests include synthetic aperture radar, ground moving target indication, and deep learning.

Yue Yang (S'17) was born in Sichuan, China. She received the B.Eng. degree in electronic engineering, in 2015, from the University of Electronic Science and Technology of China, Chengdu, China, where she is currently working toward the Ph.D. degree in electronic engineering. Her research interests include synthetic aperture radar imaging, sparse signal reconstruction, and statistical signal processing.